Journal of Geodynamics 143 (2021) 101811

Contents lists available at ScienceDirect

Journal of Geodynamics

journal homepage: www.elsevier.com/locate/jog

Another way of looking at an Alkaline Province

Elainy S.F. Martins[a,b], Roberta M. Vidotti[b,*]

[a] Instituto de Geociências, Universidade de Brasília, Brazil
[b] Universidade Federal do Oeste da Bahia, Brazil

ARTICLE INFO

Keywords:
Gravity data
Magnetic data
Forward modeling
Goiás Alkaline Province
Mesozoic
Tectonic control
Gondwana

ABSTRACT

The Mesozoic Alkaline Magmatism on the South American Platform is related to the Gondwana breakup and the opening of the South Atlantic Ocean. This event, known as the Mesozoic Activation phase, was responsible for five magmatic pulses, among them the Late Cretaceous-Eocene Alkaline Magmatism, which implemented ten alkaline provinces, eight of which are in the south-central portion of Brazil. Some authors claim that the reactivation of old zones of weakness from the Precambrian basement, Brasiliano orogeny, may have been responsible for the structuring of few bodies in these provinces. This work used geophysical processing techniques to interpret magnetic and gravity data and 2.5 D forward modeling to contribute with the knowledge on the tectonic control over the Goiás Alkaline Province. The geophysical data processing show a tectonic control over the Goiás Alkaline Province, along the Brasiliano and Mesozoic structures, and there was no predominance of alkaline bodies along the Azimuth 125. We find that the Brasiliano orogeny structures limited the crustal block that contains this Province and Gondwana breakup possibly created and reactivated these structures. We discuss the continuity of large structures, at different depths, related to the Tocantins Province, mainly in the Brasília belt, and some of them can be observed down to approximately 20 km depth. The forward gravity modeling beneath the Goiás Alkaline Province shows a thicker crust and we propose that the primitive lithospheric mantle below this province was not altered during the Brasiliano orogeny stages, as in the adjacent crustal blocks, thus allowing for generation of alkaline rocks. Along the modelled section the Arenópolis Magmatic Arc was separated into two different crustal blocks; the western arc whitin the Goias Alkaline Province, and the eastern arc where the mantle was altered due to its collision with the São Francisco Paleocontinent.

1. Introduction

The Tocantins Province (TP) (Fig. 1) is a Neoproterozoic Orogen formed by the collision of the Amazonian, São Francisco, Paranapanema paleocontinents and small allochthonous blocks (Brasiliano orogeny). This collision generated the Araguaia, Paraguay and Brasília Mobile Belts. The Brasília Belt (Fig. 2), the target of this work, is formed by External Domain, Passive Margin, Internal Domain and Goiás Magmátic Arc, were is located the Goiás Alkaline Province (GAP), a Mesozoic Alkaline Province, the focus of this work (Fig. 2) (Fuck et al., 2014, 2017; Pimentel and Fuck, 1992, 1994; Pimentel et al., 2000a, 2000b; Pimentel, 2016; Valeriano et al., 2008).

The External Domain comprises Araí, Paranoá and Bambuí groups (Fuck et al., 2014; Pimentel, 2016) (Fig. 2). Cordeiro and Oliveira (2017) observed that the geological units of the Cavalcante-Natividade Block are similar to the units of the Goiás Massif, showing no evidence of syn-collisional magmatism. According to the authors, this block is part of the Goiás Massif, being classified as Cavalcante-Arraias Domain, whose amalgamation occurred in the Paleoproterozoic. The Passive Margin is formed by Vazante, Paranoá, Canastra, Andrelândia, and Ibiá Groups (Fuck et al., 2014; Pimentel, 2016; Pimentel et al., 2004; Valeriano et al., 2004, 2008) (Fig. 2). The Internal Domain comprises the Metamorphic Core and the Goiás Massif (Fuck et al., 2014; Pimentel, 2016). Cordeiro and Oliveira (2017) subdivided the Goiás Massif into the Crixás-Goiás, Campinorte and Cavalcante-Arraias Domains (Fig. 2). The Goiás Magmatic Arc is divided into Mara Rosa (northern) and Arenópolis (south-southeastern) Magmatic Arcs (Cordeiro and Oliveira, 2017; Fuck et al., 2008, 2014; Laux et al., 2005; Pimentel and Fuck, 1994; Pimentel et al., 2000a, 2000b; 2004; Pimentel, 2016; Valeriano et al., 2008) (Fig. 2).

The GAP is located on the western edge of the Arenópolis Magmatic Arc, NNE of the Paraná basin (Fig. 2, blue dashed polygon), represented by dunites, clinopyroxenites, peridotites, alkali gabbro, trachyte, among others, dated between 88–90 Ma (Almeida, 1983; Brod et al., 2005;

* Corresponding author.
E-mail addresses: elainy.martins@ufob.edu.br (E.S.F. Martins), roberta@unb.br (R.M. Vidotti).

https://doi.org/10.1016/j.jog.2020.101811
Received 24 April 2020; Received in revised form 16 November 2020; Accepted 1 December 2020
Available online 8 December 2020

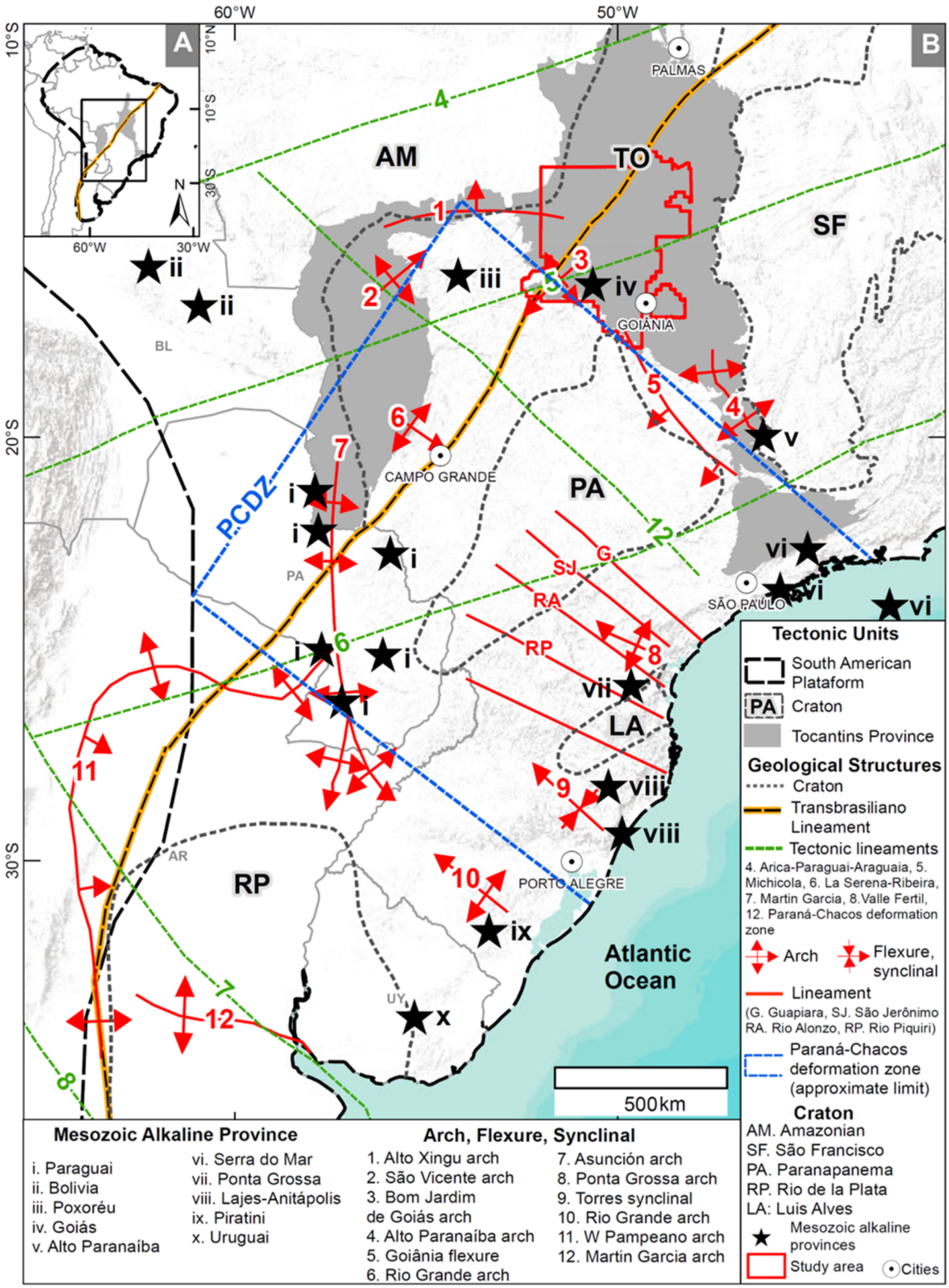

Fig. 1. Map showing the Tocantins Province in the South American Platform (A). Mesozoic alkaline provinces map and associated tectonic structures (B). **PCDZ** Paraná-Chacos Deformation Zone (blue dashed line) (adapted from Almeida et al., 1981; Almeida, 1983, 1986; Bizzi et al., 2003; Brod et al., 2005; Cernuschi et al., 2015; Comin-Chiaramonti and Gomes, 1996; Comin-Chiaramonti et al., 2005; Cordani et al., 2016; Gibson et al., 1995, 1997, 1999; Gomes et al., 1990; Jacques, 2003a, 2003b; 2004; Kirstein et al., 2000; Lagorio, 2008; Lustrino et al., 2005; Matton and Jébrak, 2009; Peyve, 2010; Riccomini et al., 2005; Thompson et al., 1998; Ulbrich and Gomes, 1981; Velázquez et al., 1996) (For interpretation of the references to colour in this figure legend, the reader is referred to the web version of this article.).

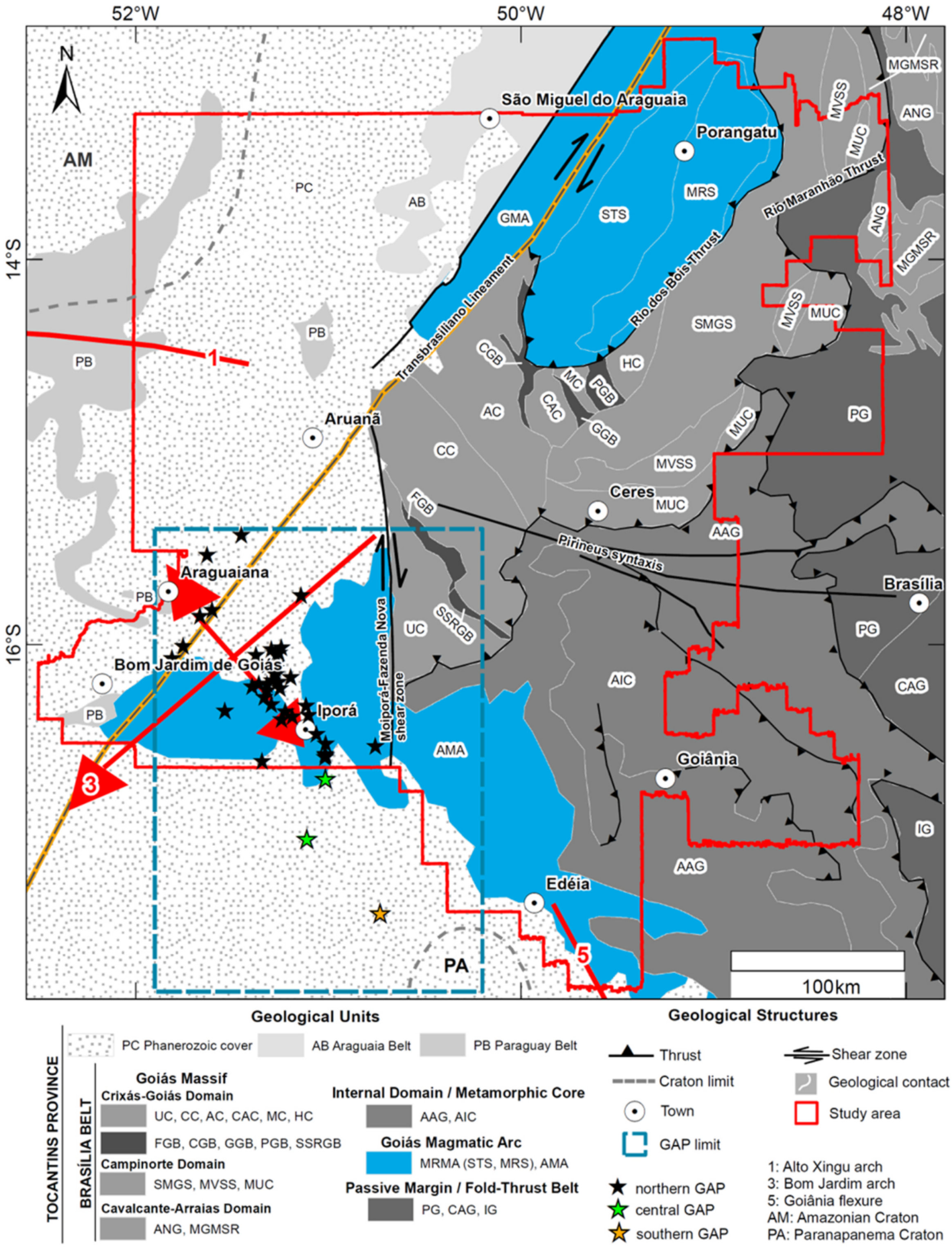

Fig. 2. Geological units of the Tocantins Province highlighting the Goiás Magmatic Arc (**GMA**) (blue polygon) and Goiás Alkaline Province (**GAP**) (blue dashed polygon). Brasília Belt: **UC** Uvá Complex, **CC** Caiçara Complex, **AC** Anta Complex, **CAC** Caiamar Complex, **MC** Moquem Complex, **HC** Hidrolina Complex, **FGB** Faina Greenstone Belt, **CGB** Crixás Greenstone Belt, **GGB** Guarinos Greenstone Belt, **PGB** Pilar Greenstone Belt, **SSRGB** Serra de Santa Rita Greenstone Belt, **SMGS** Serra da Mesa Group/Suite, **MVSS** Metavulcano Sedimentary Sequence, **MUC** Mafic Ultramafic Complex, **ANG** Araí/Natividade Groups, **MGMSR** Metagranite and Metasedimentary Rocks. **AAG** Araxá/Andrelândia Groups, **AIC** Anápolis-Itauçu Complex. **MRMA** Mara Rosa Magmatic Arc (**STS** Santa Terezinha Sequence, **MRS** Mara Rosa Sequence), **AMA** Arenópolis Magmatic Arc. **PG** Paranoá Group, **CAG** Canastra/Andrelândia Groups, **IG** Ibiá Group (adapted from Bizzi et al., 2003; Brod et al., 2005; Cordeiro and Oliveira, 2017; Fuck et al., 2014, 2017; Fuck et al., 2008; Jost et al., 2013; Lacerda Filho et al., 2018; Oliveira et al., 2000; Pimentel et al., 2000a, 2000b, 2004; Pimentel, 2016; Valeriano et al., 2008) (For interpretation of the references to colour in this figure legend, the reader is referred to the web version of this article.).

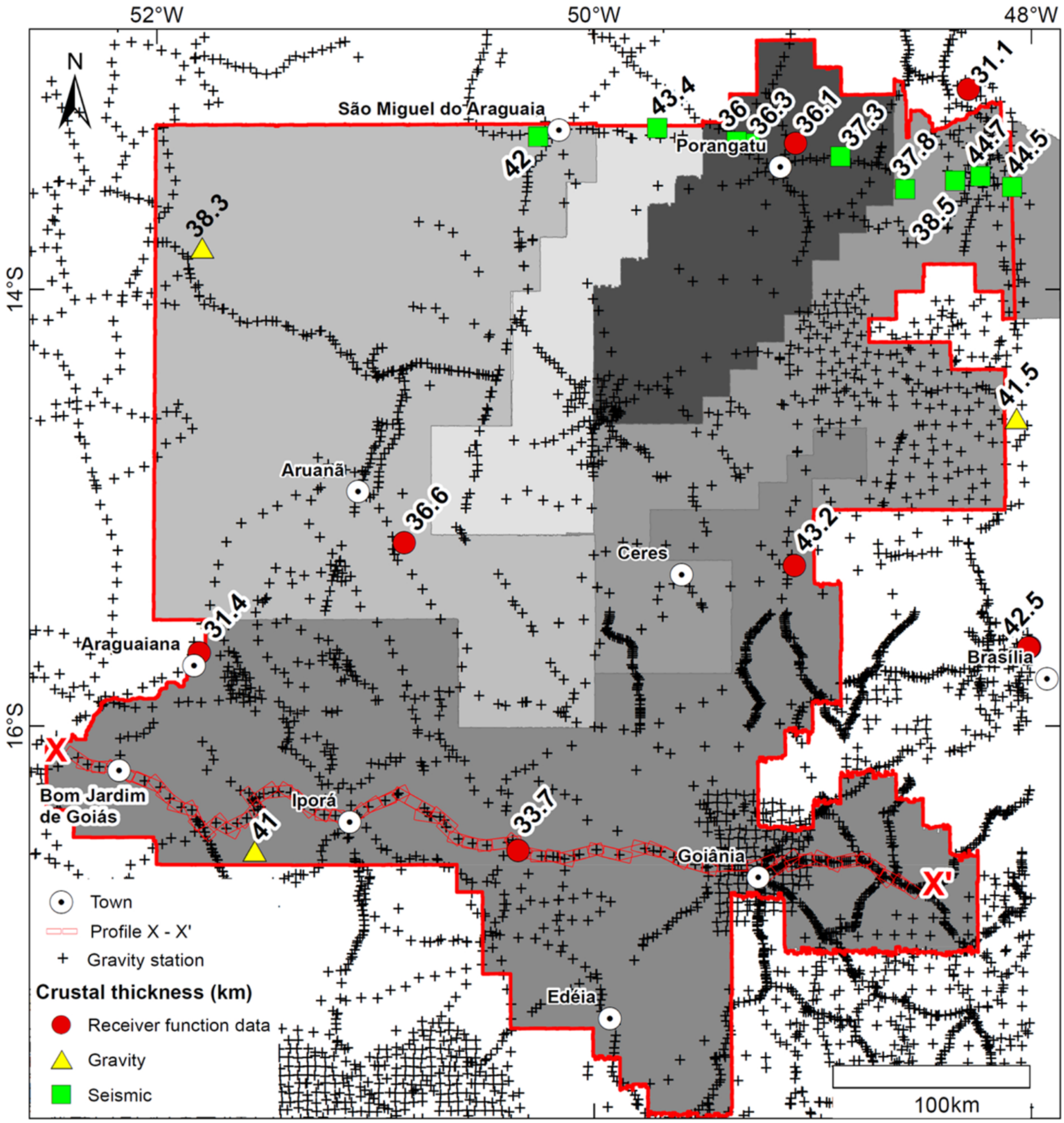

Fig. 3. Map showing the magnetic surveys in gray polygons (compiled from CPRM, 2004a, 2004b, 2005, 2012; LASA, 2006), study area (red polygon), gravity stations in black crosses (compiled from BNDG-ANP), crustal thickness (compiled from Assumpção et al., 2013; Bernardes, 2015; Pavão, 2014) and X-X' localization of the gravity profile forward modeled (red line) (For interpretation of the references to colour in this figure legend, the reader is referred to the web version of this article.).

Danni et al., 1990, 1994; Danni and Gaspar, 1994; Junqueira-Brod et al., 2005a, 2005b; Morbidelli et al., 1995; Ulbrich and Gomes, 1981).

The tectonic structures that limit the Geological Units of the Brasília Belt (Fig. 2) are still much discussed, such as the Rio Maranhão Fault, which represents the suture zone between the Goiás Massif and the São Francisco Paleocontinent (Soares et al., 2006). However, a more recent study by Cordeiro and Oliveira (2017) states that the Goiás Massif represents the western border of the São Francisco Paleocontinent while the Rio Maranhão Fault represents an intracontinental structure and not a suture zone (D'el-Rey Silva et al., 2008). In a recent work, Reis et al. (2020) affirm, from the analisys of magnetic and gravity data, that Rio Maranhão and Rio Paranã faults represent intracontinental structures agreening with previous interpretations (D'el-Rey Silva et al., 2008; Cordeiro and Oliveira, 2017). A more detailed study of the relationship of these structures with the GAP is necessary, and gravity and magnetic data can be used to verify this relationship.

The GAP and others Mesozoic Alkaline Provinces are concentrated in the south-central portion of the South American Platform, in the region named the Paraná-Chacos Deformation Zone - PCDZ, associated with arcs, flexures and tectonic lineaments (Jacques, 2003a, 2003b; 2004; Matton and Jébrak, 2009) (Fig. 1). The PCDZ is an intracontinental deformation zone formed by pre-existing basement faults that have been reactivated and accumulated stress during the Gondwana break up. In this period intra-plate reorganizations changed the intensity and direction of oceanic spreading, deep crustal movements, changing pole rotation and reactivations of ancient structures causing the alkaline magmatism that was named Paraná-Etedenka Igneous Province or Peri-Atlantic Alkaline Pulse (PAAP) (Almeida, 1971, 1966, 1983;

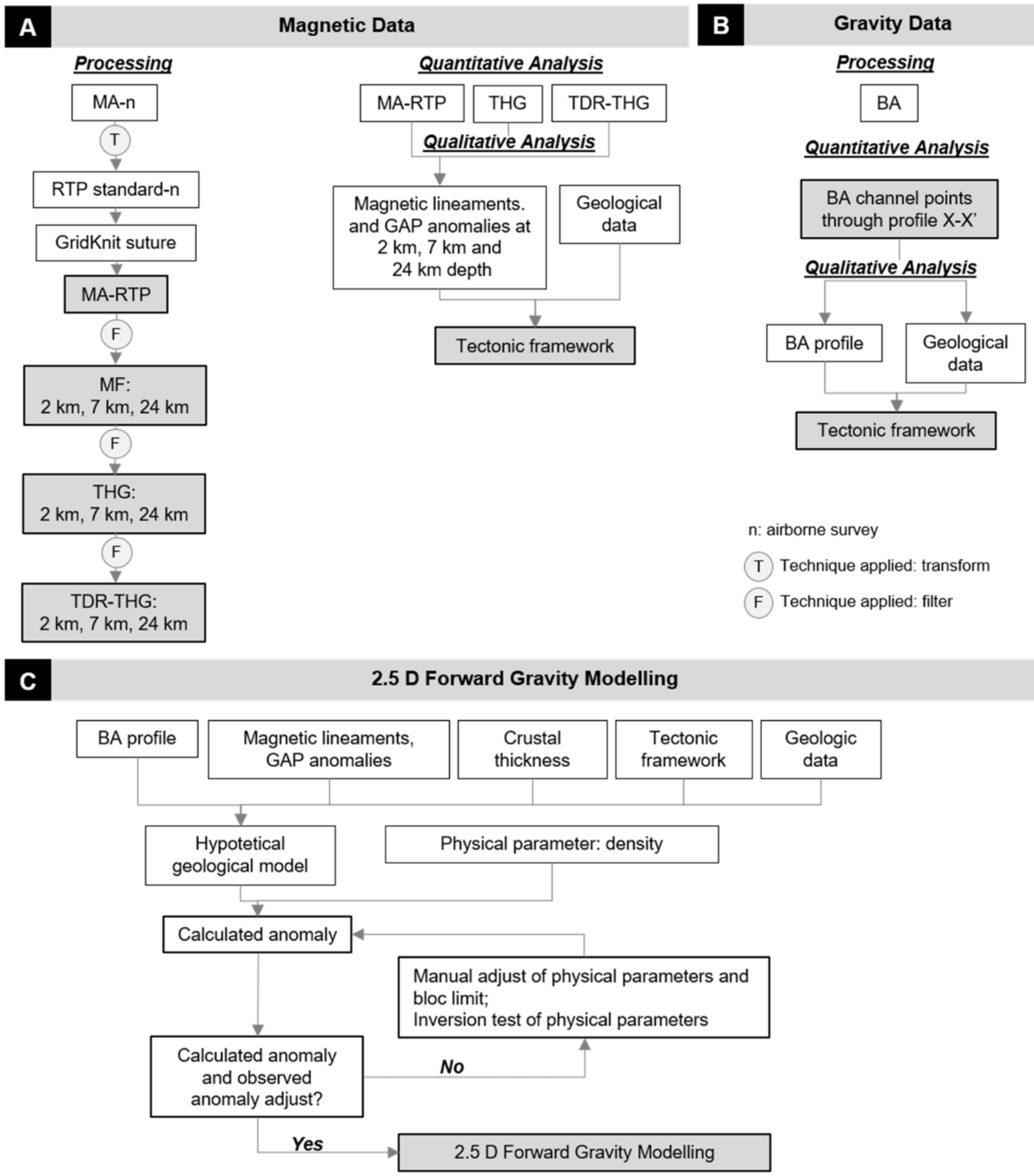

Fig. 4. Workflow chart (based on Blakely, 1996; Pinto and Vidotti, 2019; Revees, 2005). MA: magnetic anomaly, RTP: reduction to pole, MA-RTP: magnetic anomaly reduced to pole, MF: matched filter, THG: total horizontal gradient, TDR-THG: tilt derivative of the total horizontal gradient, GAP: Goiás Alkaline Province, BA: Bouguer Anomaly.

Comin-Chiaramonti et al., 1999, 2005; Gomes et al., 2018; Jacques, 2003a, 2003b; 2004; Matton and Jébrak, 2009; Riccomini et al., 2005; Sadowski, 1987). Changes in plate kinematics and seafloor spreading, opening of the Bay of Biscay – West Iberian Margin, culminated in alkaline intrusions between 105 Ma and 85 Ma in the west coast of Portugal (Miranda et al., 2009). Intracontinental rifting is also a tectono-magmatic event responsible for alkaline rocks generation, like Kola Alkaline and Carbonatite Province (380 Ma), northwestern Russia (Burke et al., 2007). On the other hand, the alkaline rocks can be generated by mantle plumes, as stated by Gibson et al. (1995, 1997, 1999) that affirm that the GAP origin is related to the Trindade Mantellic Plume.

Studies on the Brazilian Mesozoic Alkaline Provinces are mostly based on geochemical and geochronological data (Brod et al., 2005; Comin-Chaiaramoti et al., 2007; Gibson et al., 1995, 1997, 1999; Junqueira-Brod et al., 2005a, 2005b; Matton and Jébrak, 2009). Although there are also works based on geophysical data (Dutra and Marangoni, 2009; Dutra et al., 2012, 2014; Feitoza, 2011; Marangoni and Mantovani, 2013; Mantovani et al., 2015; Marangoni et al., 2015; Oliveira et al., 2015; Rocha et al., 2014, 2015, 2019a, 2019b), but, there is no specific work on the tectonic structure generated during the Brasiliano orogeny and the possible relationship of the Arenópolis Magmatic Arc and GAP.

The Arenópolis Magmatic Arc is the result of the crustal accretion of two arcs, the older arc is located in the west portion, is represented by orthogneisses and granitoids with emplacement ages between ca. 821 Ma and 782 Ma and the younger arc is located in the east portion of the Arenopolis Magmatic Arc and records the crystallization of

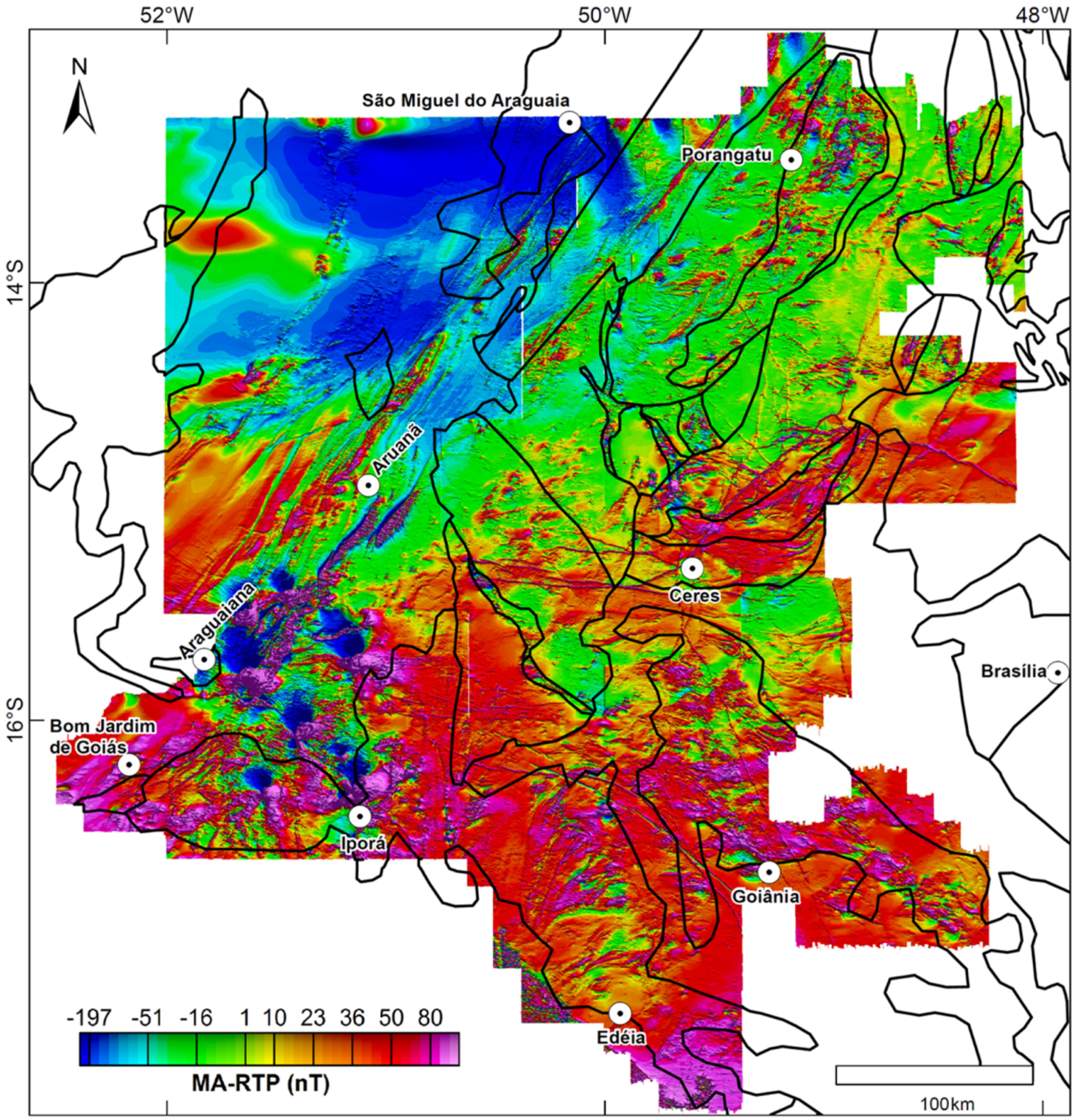

Fig. 5. Magnetic Anomaly-Reduced-to-pole map (MA-RTP). Black polygons represent the limits of the Geological Units according to Fig. 2.

metatonalites and metagranitic rocks between ca. 669 Ma and 630 Ma. However, the suture zone between these two arcs is unknown (Laux et al., 2004, 2005, 2010; Rodrigues et al., 1999). Therefore, this work proposes, based on magnetic and gravity data processing, and 2.5 D forward gravity modeling, of an E–W section, along the Arenópolis Magmatic Arc, to understand the tectonic framework of the Brasilia Belt and Arenopolis Magmatic Arc, in the context of Brasiliano Orogeny and Gondwana break up, and its relationship with the GAP.

2. Data and methods

Was used the magnetic data from five high-resolution aerial surveys (CPRM, 2004a, 2004b, 2005, 2012; LASA, 2006) provided by the Geological Survey of Brazil (CPRM) and ground gravity data provided by the Banco Nacional de Dados Gravimétricos (BNDG) - Agência Nacional do Petróleo, Gás Natural e Biocombustíveis (ANP) (Fig. 3). The gravity data used came from different surveys and different campaigns made available by various institutions, including the Instituto Brasileiro de Geografia e Estatística (IBGE), Observatório Nacional (ON), Instituto de Astronomia, Geofísica e Ciências (IAG-USP), Instituto de Geociências (IGC-USP), Universidade de Brasília (UnB) and Petróleo Brasileiro S.A. (Petrobras). These data were processed using the Oasis Montaj® (Seequent) and ArcGIS® (Esri).

The magnetic data were acquired between 2004 and 2012, have N–S flight lines with 500 m spacing, 100 m flight height, 0.1 s sampling rate for magnetometers with 0.001 nT resolution. The 2.5 D gravity forward modeling was performed using GM-SYS Profile Modeling, the crustal thickness was compiled from Assumpção et al. (2013); Bernardes (2015) and Pavão (2014). Rock physical parameters (density and magnetic susceptibility) were based on Telford et al. (1990); Reynolds (1997) and Revees (2005). Seismicity and intraplate stress was acquired from Assumpção et al. (2004, 2013), Soares et al. (2006) and Rocha et al. (2011, 2016). Geological Units used are according to Alvarenga and Trompette (1993); Bizzi et al. (2003); Fuck et al. (2014); Pimentel et al.

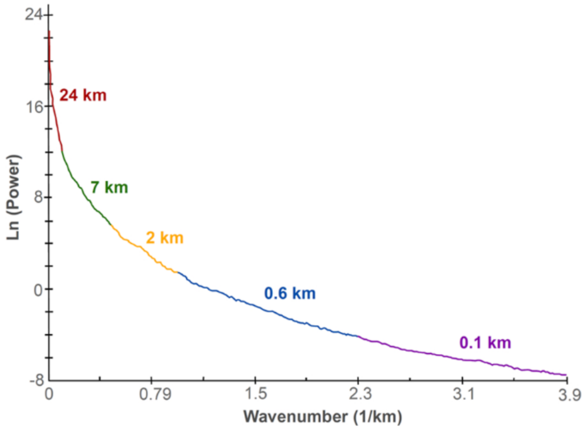

Fig. 6. Radial power spectrum from Reduced-to-pole Magnetic Anomaly, each different colored segment represents the depth to the top of different sources and its respective values.

(2000a) and Pimentel (2016), in addition to other information.

The Reduced to Pole transform (RTP) (Baranov and Naudy, 1964), the Matched Filter (MF) (Phillips, 2001), the Total Horizontal Gradient (THG) (Cordell and Grauch, 1985; Grauch and Cordell, 1987) and the Tilt Derivative of Total Horizontal Gradient (TDR - THG) (Ferreira et al., 2013) filters were used in this work (Fig. 4).

Initially, the Magnetic Anomaly (MA) was generated (MA-n), using the Bidirectional Interpolation method and 125 m cell size (Hinze et al., 2013; Isles and Rankin, 2013) (Fig. 4A). The intermediate latitude of the study area is -13 °S while the displaced from the source magnetic anomalies behave in a dipolar manner. This anomaly is common in intermediate to low latitudes (<90°) and RTP is recommended to centralize the anomalies by positioning them on the causative source (Baranov, 1957; Baranov and Naudy, 1964; Hinze et al., 2013). The MA grids reduced to the pole (RTP-n) were generated by applying RTP standard, and the magnetic field inclination (I) and declination (D), as well as inclination amplitudes, were calculated from the central coordinate and the average date of each survey (Curto et al., 2014; Hinze et al., 2013; Revees, 2005).

Only the magnetic anomalies referring to GAP were not totally centralized in this processing, which can be explained by the remnant magnetization present in these bodies (Dutra et al., 2012, 2014). This characteristic did not affect the interpretation of the referred anomalies because the work objective was to identify the number of anomalies observed at each analyzed depth. Subsequently, the RTP-n grids were joined, by the suture to each other method (Figs. 4A and 5), so the MF was applied. The MF was applied to observe the shape and continuity of magnetic anomalies, at different crustal depths, within the power spectrum (Cowan and Cowan, 1993; Hinze et al., 2013; Isles and Rankin, 2013; Phillips, 2001; Revees, 2005; Spector and Grant, 1970; Spector and Parker, 1979; Syberg, 1972). This work focus on anomalies from the deepest sources, 2 km, 7 km and 24 km depths, while the 0.1 km and 0.6 km were discarded for being related to noisy, highlighting high frequency and low depth anomalies (Fig. 6). All the depths intervals were obtained from band-pass filtering of the RTP magnetic anomaly and for the 2 km depth the wavelength intervals were 3800 m–20093 m. For the 7 km depth the wavelength intervals were 20093 m–252000 m and for the 24 km depth the wavelength greater than 252,000 m. Then THG and TDR-THG were applied (Fig. 4A).

In the qualitative analysis, the magnetic lineaments were interpreted from the MA-RTP, THG, and TDR-THG, in the three depth intervals (Fig. 4A). The magnetic lineaments may represent faults, fractures, geological contact, shear zones or dikes, and were interpreted in the 1: 2,000,000 scale, in the magnetic highs and lows, observing their continuity, following the stratigraphic principle of cross-cutting relationship. The few high-frequency N–S structures were considered as data noise and were not interpreted. Several magnetic lineaments were correlated to previously mapped geological structures, however, those that did not correlate with already mapped structures were named and are this work contribution.

The predominantly dipolar, circular, semicircular or elliptical magnetic anomalies were associated with the GAP (Fig. 4A) and interpreted in the magnetic highs of the CMA and in the center of the THG and TDR-THG (Fig. 4A). As previously mentioned, the THG and TDR-THG filters enhance the anomaly edges whereas the anomaly position in the GAP was interpreted, in this case, in the center of the circular anomalies.

The Bouguer Anomaly (BA) was interpolated from the minimum curvature, using 2000 m cell size and 5487 gravity stations (Figs. 4B and 7). In the quantitative analysis, BA values were extracted along the X-X' section and this information, together with the geological data, were used in the 2.5 D forward gravity modeling (Fig. 4B). Most of the anomalies interpreted in the work area are 2D, however, the anomalies related to the GAP have a three-dimensional (3D) character, are finite and approximately elliptical (length at least twice the width) when observed in plan. Hinze et al. (2013) stated that such characteristics allow classifying these anomalies as 2.5 D and, thus, to facilitate data interpretation and minimize the data ambiguity problem, the 2.5 D forward modeling technique was used in this work. In the 2.5D modeling, the BA information along the X-X' section, the magnetic lineaments, crustal thickness, geological database and other geological were used as input data (Fig. 4C).

A hypothetical geological model was elaborated with the possible limits of the crustal blocks while a spreadsheet was created with the physical (density) and geological parameters to feed this model and support the modeling. Geological and geophysical data (Gravity, Receive Function, Seismic Refraction data and Teleseismic P and S wave tomography) from Tocantins Province and adjacent regions were also compiled from Alvarenga and Trompette (1993); Assumpção et al. (2004, 2013), Azevedo et al. (2015); Bernardes (2015); Berrocal et al. (2004); Brod et al. (2005); Curto et al. (2014, 2015), Fuck et al. (2014); Laux et al. (2010); Macedo et al. (2018); Pavão (2014); Pimentel (2016); Pinto and Vidotti (2019); Rocha et al. (2011, 2016, 2019a, 2019b), Soares et al. (2006); Ussami and Molina (1999).

3. Results

3.1. Magnetic and gravity data

The magnetic (Figs. 5 and 8) and the Bouguer gravity (Fig. 7) anomalies were described separately for each Geological Unit (Table 1), then the magnetic lineaments were interpreted for each analyzed depth (Fig. 9).

The MA-RTP product at 2 km (Fig. 8A, D, G) shows intermediate intensity anomalies, except for the high-intensity anomalies, in the SW portion of the area, that refer to the GAP (black circle). The predominant NE-SW magnetic lineaments (Fig. 9A), have secondary NW-SE, WNW-ESE, ENE–WSW and E–W directions. Between the 15 °S and 16°30'S parallels, the NW-SE lineaments are predominant and secondarily, the NE-SW, NNW-SSE and E–W. In the area southern edge, the NE-SW lineaments predominate, followed by the NW-SE, NNW-SSE and E–W lineaments. At this depth 38 anomalies were associated with GAP (Fig. 8A, D, G).

The MA-RTP product at 7 km (Fig. 8B, E, H) show anomaly intensities vary from medium to low, while the greatest intensity contrast and highest gradients predominate in the GAP. The predominant NE-SW magnetic lineaments (Fig. 9B) have secondary NW-SE and E–W directions. At this depth 18 anomalies were associated with GAP (Fig. 8B, E, H).

The MA-RTP product at 24 km (Fig. 8C, F, I) show anomalies of low-intensity in the NW portion of the area, intermediate to low intensity in the NE portion, intermediate in the SE portion, and high in the SW portion. The high-intensity anomalies are due to the GAP, indicating the

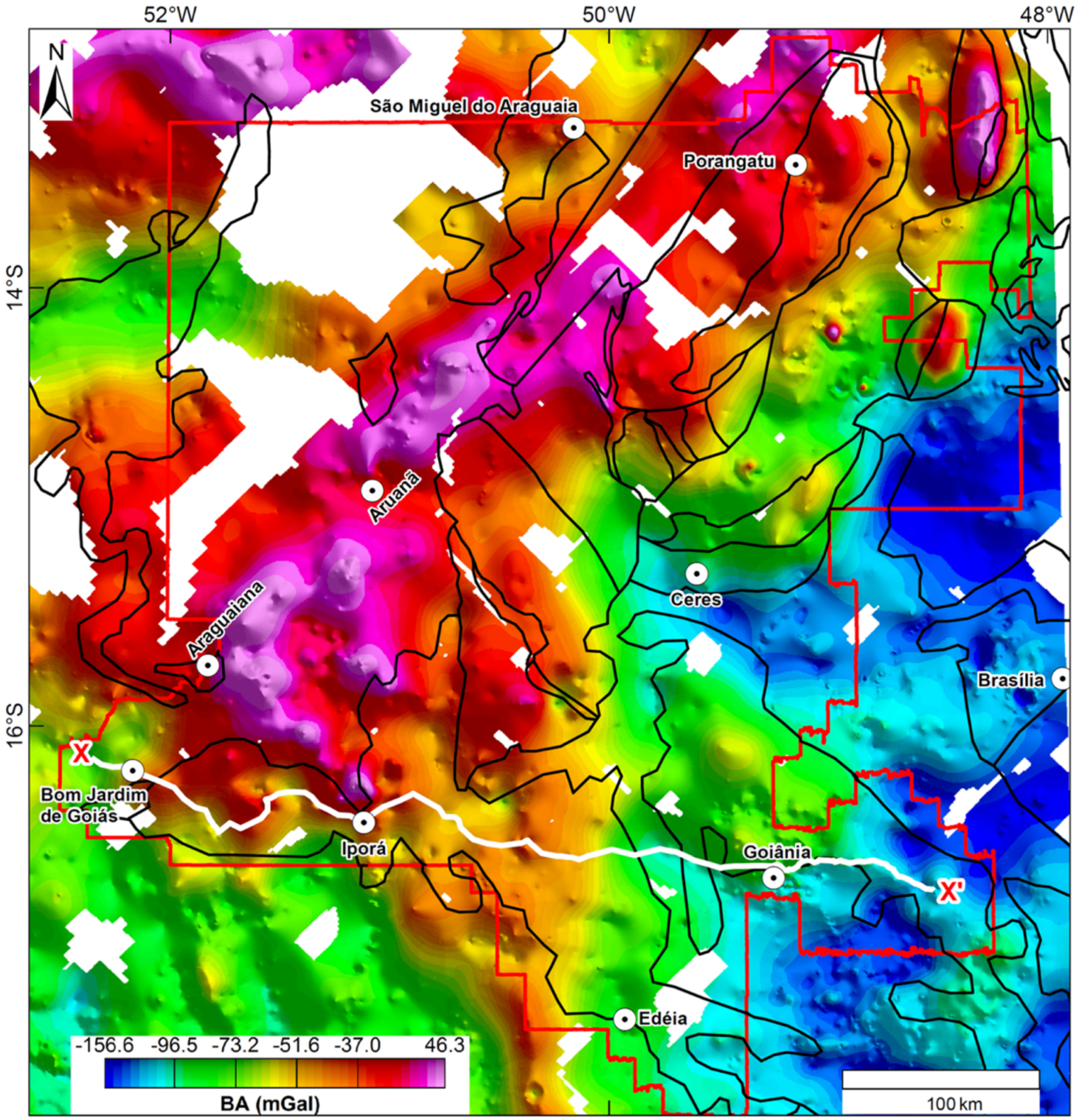

Fig. 7. Bouguer Anomaly map (BA) with gravity profile localization (X-X', white line) and study area limit (red polygon). Black polygons represent the limits of the Geological Units according to Fig. 2 (For interpretation of the references to colour in this figure legend, the reader is referred to the web version of this article.).

body responses in the analyzed depth. The magnetic lineaments (Fig. 9C) have predominant NE-SW direction, while NW-SE lineaments are observed in the central and SE portion of the area. At this depth 11 anomalies were associated with GAP (Fig. 8C, F, I).

A map of the main lineaments was generated from the joint analysis of the lineaments at the three depths (Fig. 9D) and correlated with magnetic anomaly reduced to pole map (Fig. 9E). The longest and shortest magnetic lineaments were interpreted as Major and Minor Lineaments, respectively. The Main Lineaments were numbered from 1 to 15 and correlated to mapped geological structures (Fig. 9D). In the Table 2 it is possible to identify the nomenclature and references for each structure. Furthermore, the lineaments from 16 to 54 were not identified in the bibliography and are this work contribution. The Major Lineaments were named based on their location (Fig. 9D, Table 2), the town-town lineament assigned nomenclature indicates the town closest to the beginning of the lineament and the town close to the end of the lineament, within the interpreted area.

3.2. 2.5 D forward gravity modeling

The modeling resulted in 78 crustal blocks (Fig. 10), separated by fault, shear zone or other discontinuity, according to the identified lineaments and geological structures. The Bouguer Anomaly (Fig. 10A) varies between -25 mGal and -120 mGal along the X-X' section, defining the five predominant patterns that generated the hypothetical model. The hypothetical model used information from the magnetic lineaments (Fig. 9D) assuming they represent the limits between the different crustal blocks, while the Bouguer Anomaly (Fig. 7), was associated with information on the Geological Units. The crustal thicknesses represented by the red stars (Fig. 10B) were compiled by Assumpção et al. (2013); Pavão (2014) and Bernardes (2015), whereas the crustal thicknesses of the other blocks were estimated in the modeling and compared with

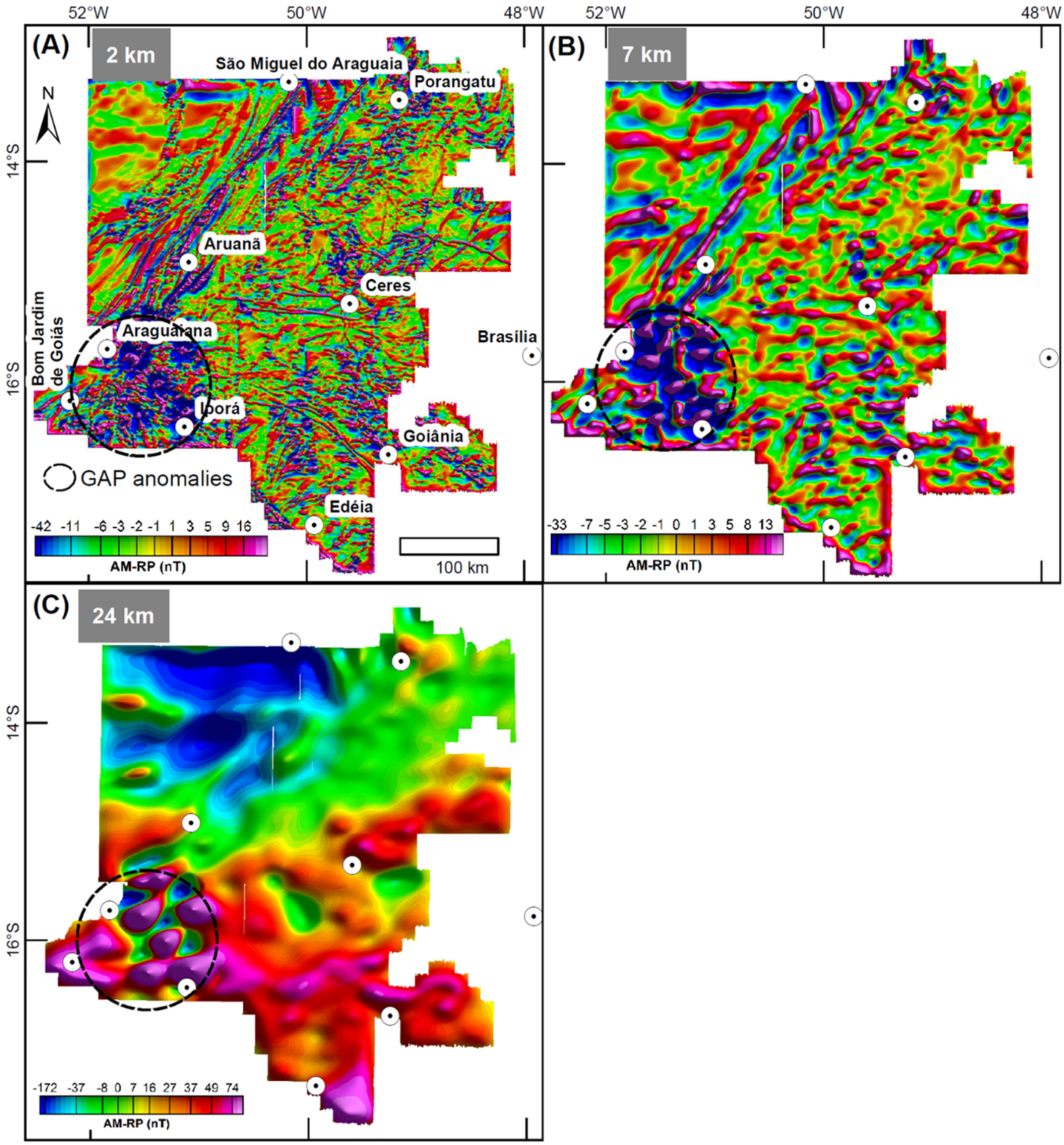

Fig. 8. Matched filter products from Reduced-to-pole Magnetic Anomaly (MA-RTP) at 2 km, 4 km and 24 km depths. Total Horizontal Gradient at 2 km, 4 km and 24 km depths. Tilt derivative from Total Horizontal Gradient at 2 km, 4 km and 24 km depths.

crustal thickness calculated in adjacent areas (Curto et al., 2015; Berrocal et al., 2004; Soares et al., 2006; Ussami and Molina, 1999).

For each Bouguer Anomaly pattern, the columns 1–5 (Fig. 10B) generated were divided into layers (A, B, C, and D), based on the varying vertical density. Column 1 was divided into three layers (A1, B1, and C1), with Bouguer Anomaly starting at -70 mGal and increasing up to approximately -30 mGal. Column 2 was divided into two layers (B2 and C2), with a predominantly constant Bouguer Anomaly pattern at -50 mGal and -25 mGal (M) peaks. Similarly, column 3 was divided into two layers (B3 and C3), with a constant Bouguer Anomaly pattern at about -60 mGal. Column 4 was divided into three layers (B4−1, B4−2, and C4), with the high Bouguer Anomaly gradient varying from -58 mGal to -100 mGal. Column 5 was divided into three layers (A5, B5 and C5), with low Bouguer Anomaly values varying between -100 mGal and -120 mGal and local high-intensity peaks (Fig. 10B).

The mean density of each block, the associated Geological Unit and the associated rock (Table 3) was used to generate the interpreted geological model (Fig. 11). Blocks A1 reach 7 km and B1 10 km depths and correspond to the upper crust. The C1 block reach 35 km depth and represent the lower crust (Fig. 10B). Block A1 was associated with Phanerozoic Cover and Paraguay Belt, and Blocks B1 and C1 were associated with the Goiás Magmatic Arc (GMA), and limited by the Serra Negra Fault to the east (Fig. 11). Block B2 has 24 km thick, represent the upper crust and locally is cut by high density blocks M. Block C2 reach 42 km depth and represent the lower crust (Fig. 10B).

Blocks B2 and C2 were associated with the Arenópolis Magmatic Arc - West (AMA-W), and was differentiated from the GMA by the Bouguer anomaly pattern, different crustal thickness, density and magnetic

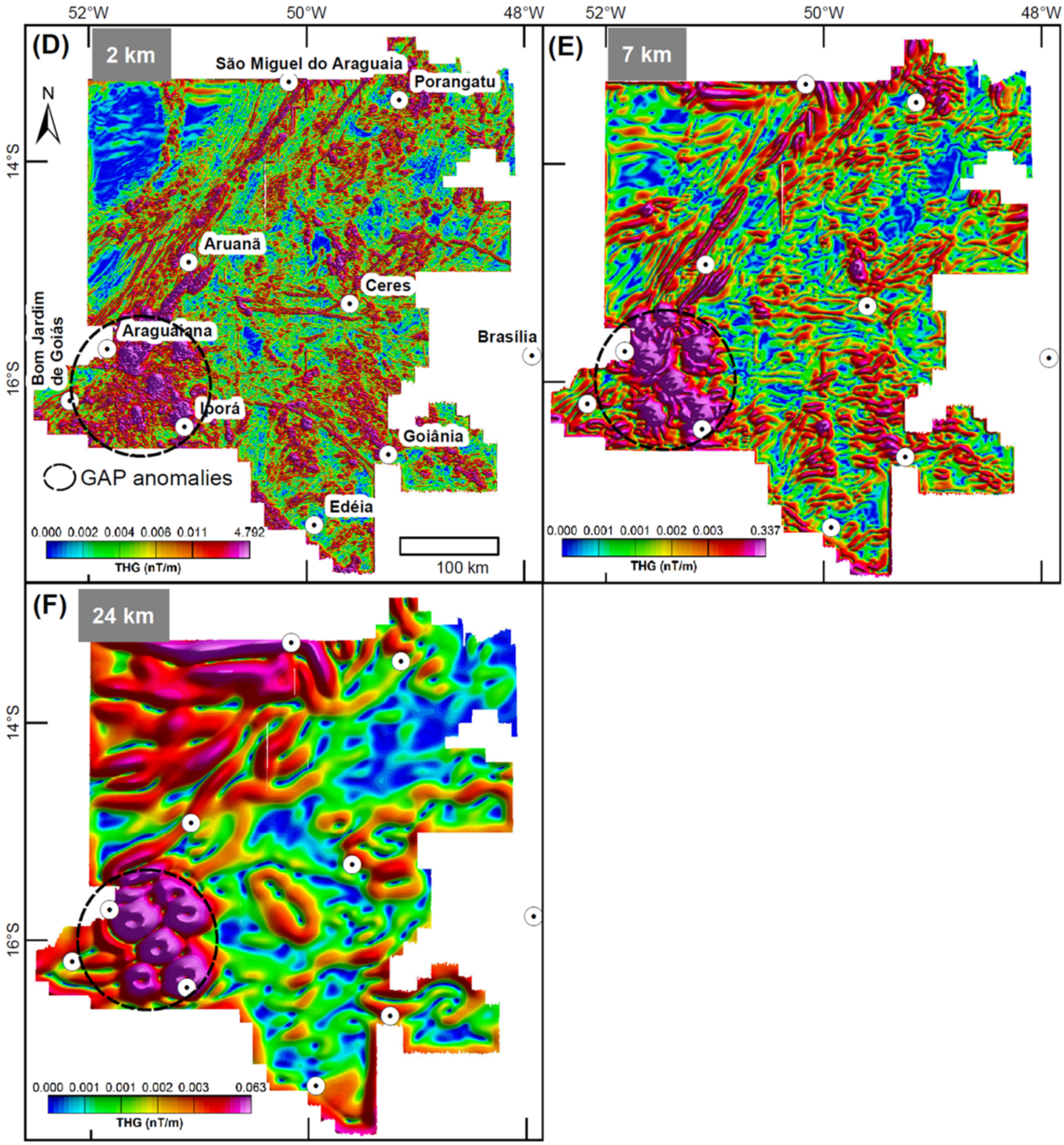

Fig. 8. (*continued*).

anomaly. Additionally, the alkaline bodies, with high Bouguer anomaly and magnetic intensities, only occur in the AMA-W (Figs. 10 and 11). High density Blocks M were associated with the Goiás Alkaline Province (GAP) and due to the proximity to mapped complexes were associated with the Arenópolis Complex (Fig. 11: 1 and 2), Fazenda Buriti Complex (Fig. 11: 3) and Morro do Macaco Complex (Fig. 11: 4). According to our modeling, a large volume of this high-density rock is located in the lower crust and may have been the source of the complex 1–4. The AMA-W eastern edge is marked by the Moiporá-Fazenda Nova Shear Zone (Fig. 11).

Block B3 has about 24 km thick and represent the upper crust. C3 block reach 34 km depth, represent the lower crust (Fig. 10B) and has crustal thickness lower than the AMA-W. Also, unlike the AMA-W, the AMA-E does not exhibit high-intensity Bouguer anomaly peaks and high magnetic anomaly. The AMA-E eastern limit is the Anicuns-Palmeiras Lineament, which represents, in the subsurface, the suture zone between AMA-E and the São Francisco Paleocontinent (SFPC) (Fig. 11).

Blocks B4−1 and B4−2 reach about 23 km thick and represent the upper crust. Block C4 reach 38 km depth and represent the lower crust (Fig. 10B). Based on the density values and geological information, Block B4−1 was also correlated to AMA-E, but as the block thickness and extension decreased to the east, we hypothesized that this block is partially covered by Block A5. The Block B4−2 may represent portions of Araxá/Andrelândia Groups (AAG) and Anápolis-Itauçu Complex (AIC) that were partially covered by AMA-E. In addition, a large part of block B4−2 and Block C4 were associated with SFPC due to the lower average densities compared to AMA-E. These geological units of different densities and thicknesses, together with the suture zone between AMA-E and SFPC, in-depth, caused a strong gradient in the Bouguer anomaly pattern over this region of the X-X' section (Figs. 10 and 11).

Blocks A5 has 7 km thick, B5 has 17 km thick and represent the upper

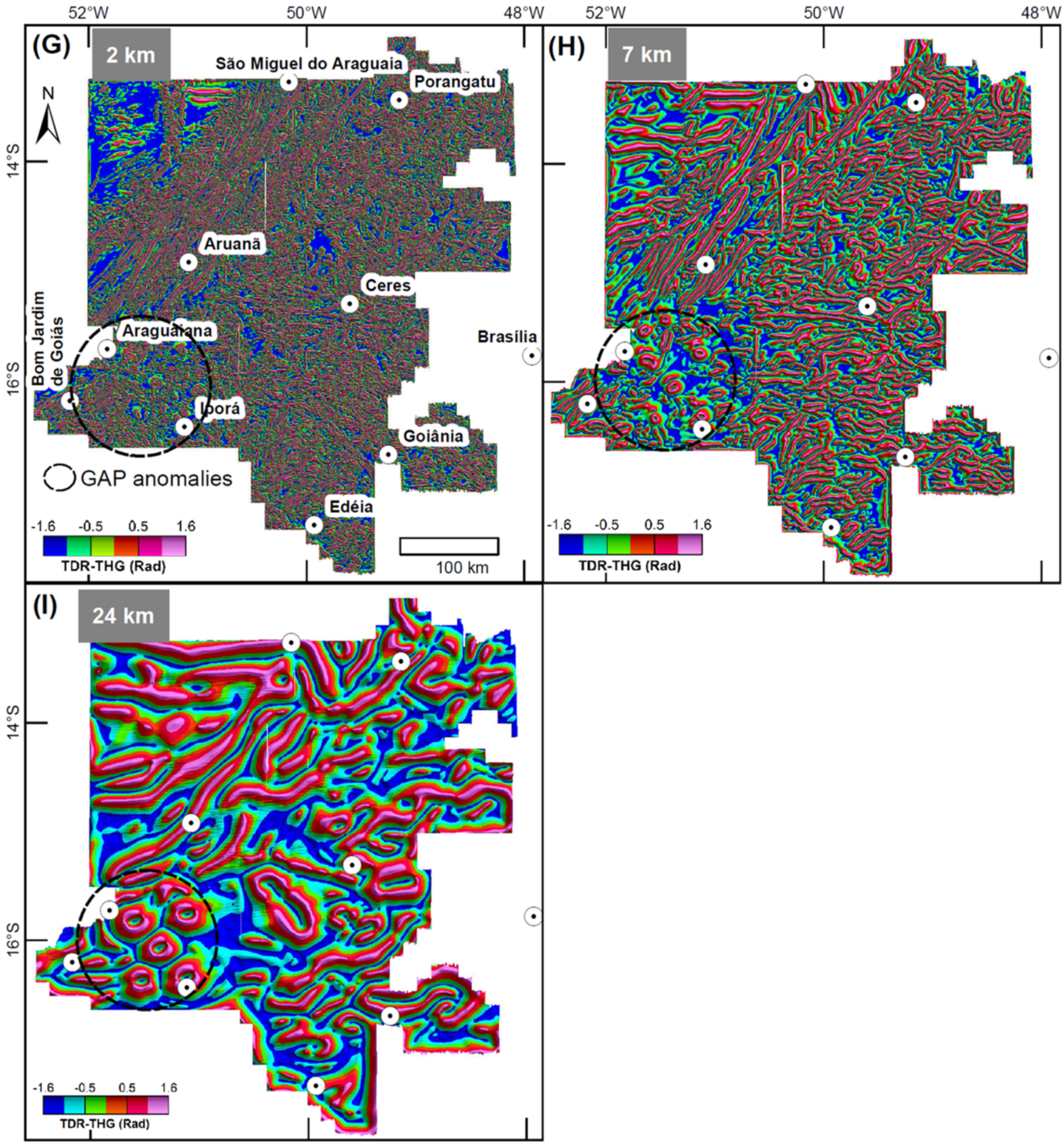

Fig. 8. (*continued*).

crust. Block C5 reach 38 km depth and represent the lower crust. (Fig. 10B). Block A5 was correlated to AAG and AIC, while the varying rock density of these units caused the Bouguer Anomaly to vary greatly over this region and, possibly, the lower Bouguer anomaly values reflect the lower density rocks of the AAG, while the Bouguer anomaly peaks reflect the high-grade metamorphic rocks of the AIC. The B5 and C5 blocks were associated with the SFPC (Fig. 11). Block D has a variable thickness and corresponds to the mantle (Fig. 10B).

4. Discussion

4.1. Magnetic lineaments and GAP relationship

The structures were separated into eight possible formation phases (Fig. 12A through H) based on the cross-cutting relationship and in the evolution of the Tocantins Province. This allowed to verify the relationship of the structures with the GAP (Fig. 9D).

The initial phase (Fig. 12A) affected the Crixás-Goiás Domain and formed Lineaments (41) (NW-SE) and (51) (NE-SW). Lineament (41) is parallel to the Faina and Serra de Santa Rita Greenstone Belts, marking the boundary between the Uvá and Caiçara Complexes (Figs. 12A and 2), and may represent the structure that gave rise to these Greenstone Belts or the suture between the Complex Uvá (Archean) and the other Archean complexes to the north. The collage between the terrains of the Crixás-Goiás Domain occurred before the Brasiliano orogeny (Cordeiro et al., 2014; Jost et al., 2005, 2013). The Uvá Complex represents a terrain formed independently of the terrains in the northern portion of the Crixás-Goiás Domain and, possibly, comes from fragments of the Amazonian or Paranapanema Paleocontinent (Jost et al., 2013).

Later (Fig. 12B) the NE-SW GPL (19), CML (20) and RMF (13) structures were generated during the formation of the Campinorte Domain, being later cut by the WNW-trending GMGL (24), which

Table 1
Magnetic and Gravity anomaly interpreted in the Geological Units of the study area (Geological Units detail see Fig. 2.

Geological Unit	Magnetic anomaly response	Gravity anomaly response
External domain	*This work assumes that the Cavalcante Natividade block is part of the Goiás Massif outside the study area.	
Passive Margin	**Fold-thrust belt:** outside the study area.	**Fold-thrust belt:** low-intensity anomalies are predominant (< -100 mGal).
	Metamorphic core **AAG:** intermediate to high-intensity anomalies (- 4 to 50 nT). **AIC:** high-intensity anomalies (50 to 1000 nT).	**Metamorphic core** **AAG:** intermediate to low-intensity anomalies (-63 to -100 mGal). **AIC:** intermediate intensity anomalies are predominant (-63 to -100 mGal).
Internal Domain	**Goiás Massif** **CGD:** intermediate intensity anomalies predominate (7 to - 33 nT), high-intensity anomalies observed at UC (30 a 100 nT), greenstone belts and MUC. **CD:** intermediate intensity anomalies (- 30 to 10 mGal), high-intensity anomalies observed at MUC (10 a 30 nT).	**Goiás Massif** **CGD:** intermediate intensity anomalies are predominant (10 to -63 mGal). **CD:** intermediate intensity anomalies (-80 to -50 mGal), high-intensity anomalies observed at some MUC (> 10 mGal).
Goiás Magmatic Arc	**CAD:** outside the study area. **MRMA:** intermediate to low-intensity anomalies (7 to – 200 nT). **AMA:** intermediate to high-intensity anomalies (> 17 nT).	**CAD:** outside the study area. **MRMA:** intermediate to high-intensity anomalies (> -40 mGal). **AMA:** intermediate to high-intensity anomalies (> -40 mGal).

extends to the vicinity of Ceres city, following almost parallel to the eastern limit of the Crixas-Goiás Domain. The Campinorte Domain was affected by two deformational events (Cordeiro et al., 2014; Cordeiro and Oliveira, 2017) and because these structures, as well as the structures observed in the Crixás-Goiás Domain, were identified only in the Goiás Massif, we believe that they may be related to these events that occurred between 3.10 Ga to 1.25 Ga (Cordeiro and Oliveira, 2017).

The Goiás Massif were amalgamated before the Brasiliano orogeny and represent a peripheral portion of the SFPC (Cordeiro et al., 2014; Cordeiro and Oliveira, 2017) whereas the RMF (13), assigned as a suture zone between GM and SFPC, represents an intracontinental structure (D'el-Rey Silva et al., 2008). The structures in Fig. 12A and B were interpreted as representing Pre-Brasiliano features and when associated with the anomalies of the alkaline complexes, indicate no relationship among them.

Between 0.8 Ga and 0.5 Ga, Brasiliano orogeny, four orogenetic pulses affected the Tocantins Province and in the final phase of this Orogeny, the extensive NE and NW shear zones developed (Almeida et al., 2000; Araújo Filho and Kuyumjian, 1996; Brito Neves et al., 2014; Brito Neves and Fuck, 2013; Pimentel et al., 2000a; Pimentel, 2016; Viana et al., 1995) may have been responsible for the structures identified in Fig. 12C, D, E and F.

We believe that the collision between the GMA and the GM formed the NE-SW XL (7), GCF (3), SNF (6), TBL (8), UPL (27), RBF (12), AML (16), APL (15), PIL (44) structures, and lineament (35) (Fig. 12C), and since these structures only affected the GMA, they were, therefore, associated with this collision event between 0.8 Ga to 0.77 Ga (Brito Neves and Fuck, 2013; Cordeiro and Oliveira, 2017; Pimentel et al., 2000b).

After this phase, HAL (18) was formed intercepting the structures observed in the northern portion of GMA (numbers 12, 27, 8 - Fig. 12C) and the eastern edge of the Crixás-Goiás Domain (number 24 - Fig. 12B). Subsequently, the BHF (4) and SLMBSZ (14) structures were formed and limited by HAL (18), and MFNSZ (10a) and MNBSZ (10b) were formed as well, limited by BHF (4) (Fig. 12D). Possibly, in this same phase, the NE-SW structure NXNPL (28) (Fig. 12E) was formed, intercepting the structures in the northern portion of the GMA (numbers 6, 8, 12, 27 - Fig. 12C).

Rodrigues et al. (1999) believed that MFNSZ (10a) and MNBSZ (10b) could represent an extension of TBL (8) however, based on the data analysis (Fig. 8) these structures are limited by BHF (4) to the north and do not connect to the TBL (8). MFNSZ represents an important discontinuity within GMA and between GMA and GM (Motta-Araújo and Pimentel, 2003).

The predominantly NW-SE structures highlighted in Fig. 12F intersect or are limited by the structures identified in Fig. 12C and D, related to the initial orogenetic pulses of the Brasiliano orogeny, being, therefore, associated with its final event (Brito Neves et al., 2014; Brito Neves and Fuck, 2013). At the end of the Brasiliano orogeny extensive tectonics was predominant in Western Gondwana due to the stabilization and collapse of the orogenic belts, and also due to the reflex of the compressive tectonics of Pampeana Orogeny (Cordani et al., 2013). In this period tectonic conditions favored the formation of dike systems, such as Azimuth125 (11), which intercepts the southern portion of the study area (Fig. 12F).

Azimuth 125 represents dike systems dated between 790 Ma and 118 Ma (Rocha et al., 2014, 2019a, 2019b) and possibly was reposnible for the tectonic control of alkaline magmatism in the Goiás Alkaline Province and in the others Brazilian Mesozoic alkaline provinces (Dutra et al., 2014; Marangoni and Mantovani, 2013; Rocha et al., 2014, 2015, 2019a, 2019b). After interpreting the magnetic data Rocha et al. (2019a, 2019b) reported that Azimuth 125 was not observed in the Mato Grosso and Rondônia states and concluded that this structure does not extend much west of the TBL, however, they were unable to detail the reason for its non-continuity.

As interpreted in this study it was noticed that part of Azimuth 125 (11) and FNAL (23) were partially displaced from the NW-SE to the NE-SW direction, and possibly continue under the Paraná Basin. The Azimuth 125, in the west of the TBL, occurs up to the vicinity of Campinápolis (Mato Grosso state), represents second and third-order shallow magnetic lineaments (Silva, 2018). However, this structure continuity into the Paraná Basin domain was not observed in the works by Pinto and Vidotti (2019) and Curto et al. (2015).

We believe that these structures were displaced due to reactivations of MFNSZ (10A) or HAL (18) (Fig. 12F). RMF (13) also displaces part of Azimuth 125 (11) such characteristics clarify the reason for the whole non-continuity of Azimuth 125 (11) in the west of TBL (8) (Figs. 9D and 12 F). Based on the cross-cutting relationship the Azimuth 125 were probably formed at the end of the Neoproterozoic and beginning of the Phanerozoic (Fig. 12F), and has estimated depth between 2 km and 7 km in the study area (Fig. 9A and B).

In the Mesozoic, during the Activation phase of the South American Platform, vertical movements predominated forming flexures and arcs (Almeida et al., 2000), such as the Alto Paranaíba, Rio Grande and Bom Jardim de Goiás Arcs, wich is located in the SW portion of the work area. The arches, as well as the reactivations of the TBL and other structures, played an important role in the emplacement of the alkaline intrusions (Almeida et al., 2000; Brito Neves and Cordani, 1991; Pena and Figueiredo, 1972).

The structures identified in Fig. 12G were associated with the Mesozoic (newly formed or reactivated) because they occur in the vicinity of the TBL and Bom Jardim de Goiás Arc, intersecting the lineaments PAL (26), (39), (38) and Azimuth 125 (11) (Fig. 12F). These are located predominantly in the AMA western edge with prevalent NE-SW direction while a large part is bounded by the BHF (4) to the north.

Several authors reported a high concentration of alkaline bodies throughout Azimuth 125 (Biondi, 2005; Bizzi and Araújo, 2005; Dutra et al., 2014; Marangoni and Mantovani, 2013; Mantovani et al., 2015;

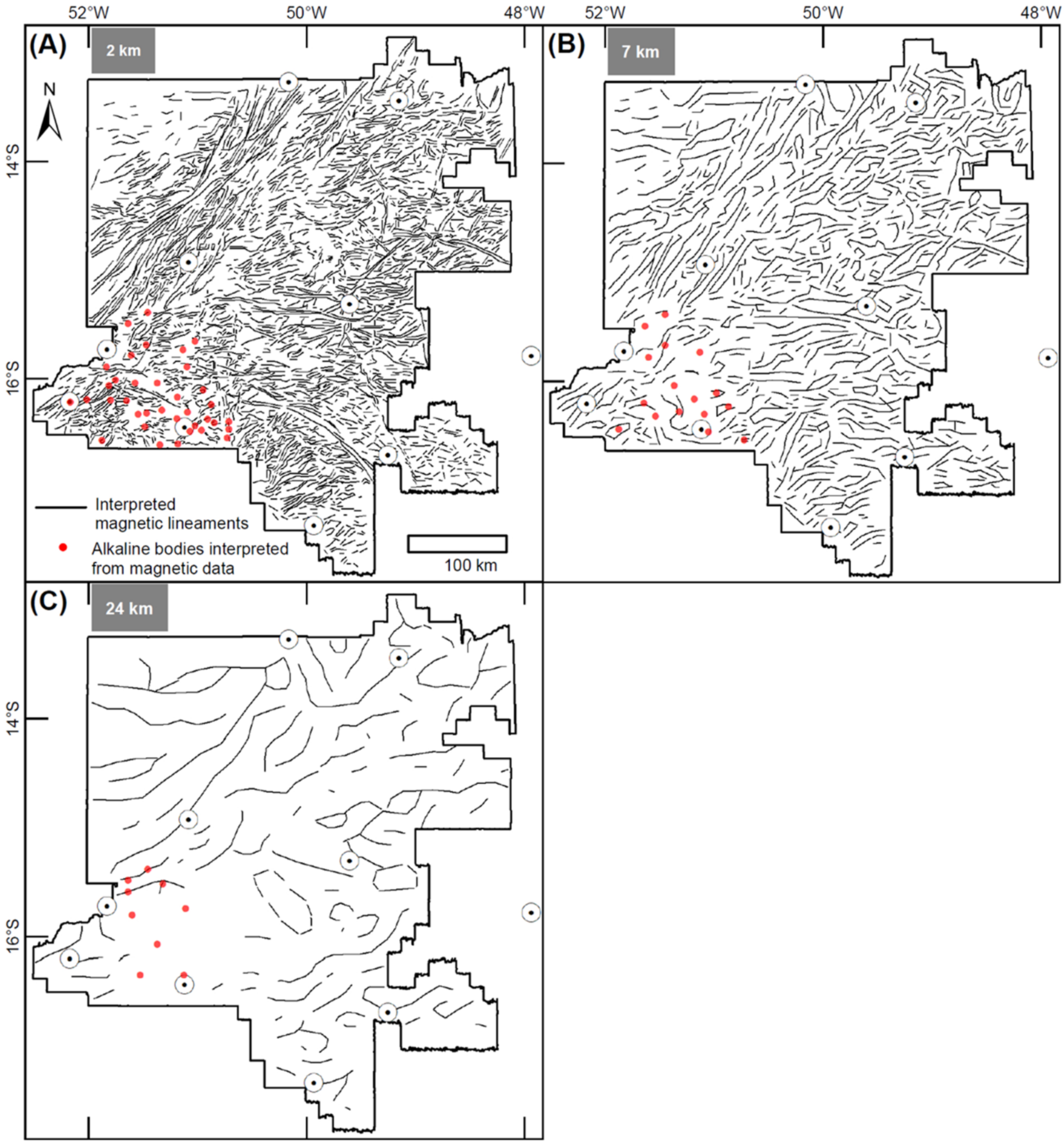

Fig. 9. Magnetic lineaments and alkaline bodies interpreted at 2 km (A), 4 km (B) and 24 km (C) depths. Map of major (numbered 1 to 54) and minor magnetic lineaments (not numbered) with kinematic interpretation, including all alkaline bodies interpreted at all depths (D). X-X' represent the profile modeled. Magnetic anomaly reduced to pole map and major lineaments (E). See Table 2 for magnetic lineament nomenclature details.

Rocha et al., 2014, 2015, 2019a, 2019b), however, our analysis indicated no preferable concentration of the GAP along the Azimuth 125 trend.

Furthermore, in the western edge of the AMA, limited by structures formed during the Brasiliano orogeny (Fig. 12C and D), a large concentration of alkaline bodies has been mapped and interpreted in the NW-SE and NE-SW structures generated in F and G phases, so we believe that the emplacement of GAP occurred preferably in the vicinity of structures generated at the end of the Brasiliano orogeny and the Mesozoic structures.

In the Cretaceous, Pena and Figueiredo (1972) state that the SW portion of the study area was affected by N50W gravity faults, forming a sequence of horsts and grabens, over 120 km long and 50 km wide. Pre-Cambrian structures were reactivated, and the emplacement of the alkaline magma occurred preferentially at the crossing of these structures (CPRM, 1974; Ohofugi et al., 1976; Pena and Figueiredo, 1972; Pena, 1975). Subsequently, the NE structures were reactivated and displaced some bodies of the GAP.

In the last phase (Fig. 12H), the formed E–W structures cross-cutting all the previously formed structures NXML (22), UAL (46), AJL (21), and SVL (5). These structures, of which many are seismogenic, were associated with Neotectonic activities (Hasui, 2010; Riccomini and Assumpção, 1999) (Fig. 13).

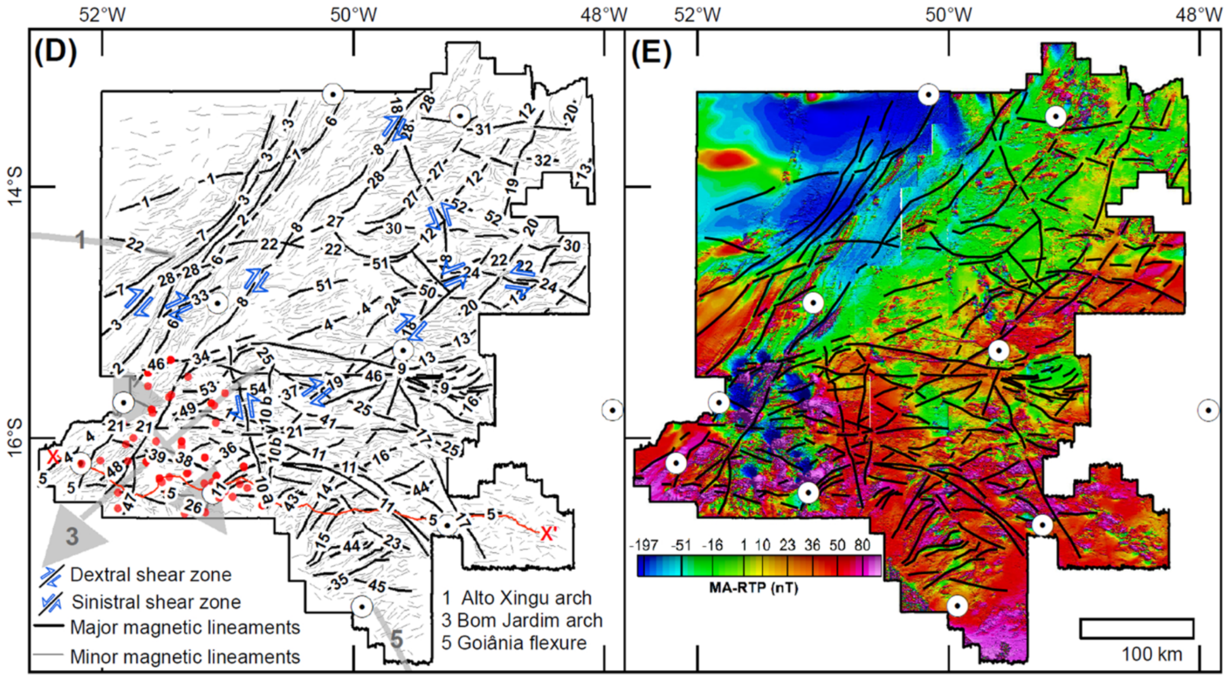

Fig. 9. (*continued*).

4.2. 2.5 D forward gravity modeling, arenópolis magmatic arc and GAP relationship

Along the X-X' section (Fig. 11) we identified the Paraguay Belt (PB), Phanerozoic Cover (PC), Goiás Magmatic Arc (GMA), Arenópolis Magmatic Arc - West (AMA-W), Goiás Alkaline Province (GAP), Arenópolis Magmatic Arc - East (AMA-E), Araxá and Andrelândia Groups (AAG), Anápolis Itauçu Complex (AIC) and São Francisco Paleocontinent (SFPC).

The PB and PC (Fig. 11) were modeled within the same block because well data were not available to used in this modeling. The gravity (Fig. 7) and magnetic (Fig. 5) data, as well as the geological model (Fig. 11), indicate that the geological unit under PB and PC, west of TBL (8), and west of SNF (6) until to the GCF (3) vicinity, represents the continuity of the GMA, while the GCF (3) represents the suture between the GMA and the Amazonian Paleocontinent (APC) (Fig. 13).

GMA (Fig. 11) extends to NE and SW (Pimentel, 2016) and represents the gravity low parallel to the TBL, under the Paraná Basin (Pinto and Vidotti, 2019). The intermediate to low intensity magnetic anomalies (Fig. 5) probably reflect the less magnetic rocks occurring above the GMA (Paraguai and Araguaia Belts, and PC). The Bouguer anomaly varies from intermediate to high (Fig. 7) in the GMA outcropping portion (near Porangatu), while the high values observed in the non-outcropping along NE-SW can be the response of rocks with higher density contrast. The GAP were not identified in the GMA. The predominantly NE-SW magnetic lineaments are observed up to 24 km (Fig. 8: G, H, I), partially coinciding with the occurrence of earthquakes (Fig. 13). On the other hand, seismic tomography data reflect low-speed anomalies of S and P waves (Assumpção et al., 2004; Rocha et al., 2011, 2016, 2019a, 2019b).

The GMA was identified west of the TBL in the São Miguel do Araguaia (Goiás state) vicinity marking the contact with the Amazonian Paleocontinent (Berrocal et al., 2004; Soares et al., 2006). This region was individualized in the Bom Jardim and Rondonópolis Domains separated by Baliza Fault (Curto et al., 2014). The U-Pb, Sm-Nd and Lu-Hf isotopic data of Aruanã (Goiás state) and Bom Jardim de Goiás (Goiás state) show T_{DM} model ages varing between 0.86 Ga and 1.03 Ga, that indicate a isotopic signature of juvenile Neoproterozoic arc, confirm the continuity of the GMA to the west of the TBL (Ferreira, 2009). The SNF (6) is the main fault of the TBL (Curto et al., 2014, 2015) being interpreted as the suture zone between GMA and AMA-W (Fig. 13).

The AMA-W is approximately 135 km long, has the largest crustal thickness, 42 km, and is limited by the MFNSZ (10a) to the east (Fig. 11), exhibiting high intensity magnetic (Fig. 5), high gravity anomalies (Fig. 7) and circular magnetic anomalies attributed to GAP (Fig. 5).

The GAP in the section were assigned to the Arenópolis, Fazenda Buriti and Morro do Macaco Complex (Fig. 11: 1–4). The Arenópolis Complex can be represented by gabbros, nepheline syenites, clinopyroxenites, and subordinate shonkinites (Brod et al., 2005). These bodies are located near the intersection of TBL (8) and lineaments (47) and (48) (Fig. 9). The Fazenda Buriti Complex can be represented by clinopyroxenite, melagabbro, essexites, syenogabbros and syenites (Brod et al., 2005) and are located close to the PJL (36) and Lineament (38) intersection (Fig. 9). The Morro do Macaco Complex can be formed by dunites, wehrlites, olivine pyroxenites and clinopyroxenites (Brod et al., 2005) and are located close to the Azimuth 125 (11), FNAL (23) and Lineament (38) intersection (Fig. 9).

The AMA-W northern limit is marked by BHF (4) which was interpreted as the suture between AMA-W and GM (Fig. 13). This portion is marked by earthquakes (Fig. 13) and to the north of BHF (4) the magnetic data presents the predominantly intermediate anomalies (Fig. 5) characteristic of the GM. It is believed that this arc southern limit occurs underlying the Paraná basin, corresponding to the D4 and D5 geophysical domains (Pinto and Vidotti, 2019), where the gravity anomaly is predominantly low, while the magnetic anomalies are intermediate to high with anomalies characteristic of the GAP.

The MFNSZ (10a) marks the eastern limit of the AMA-W (Fig. 13) and continues toward the south, turning SE where it connects with the Flexura de Goiânia (Pinto and Vidotti, 2019). Some lineaments are not observed in AMA-E, such as PJL (36), PAL (26) and lineaments (38), (39), (48) (Fig. 9).

Currie depth is predominantly greater than 49 km (Rocha et al., 2019a, 2019b) in agreement with the greater crustal thickness of this block (Assumpção et al., 2013; Bernardes, 2015; Pavão, 2014). There are few heat flow stations in the area, however, in general, the heat flow is lower over AMA-W and increase to the east of the X-X' profile modeled (Alexandrino and Hamza, 2007; Hamza et al., 2005, 2020). The anomalies of S and P waves have relatively lower speeds than those observed

Table 2
Nomenclature of major magnetic lineaments. The bold numbers and nomenclature are contribution of this study.

Lineament number	Nomenclature (Prefix)	Source
1	Campinápolis Lineament (CL)	Silva (2018)
2	Barra do Garças Lineament (BGL)	Sousa (2017)
3	General Carneiro Fault (GCF)	Curto et al. (2014, 2015)
4	**Baliza-Hidrolina Fault (BHF)**	Adapted from Curto et al. (2014, 2015)
5	São Vicente Lineament (SVL)	
6	Serra Negra Fault (SNF) (main TBL fault)	Curto et al. (2014, 2015)
7	Xambioá Lineament (XL)	Sousa (2017)
8	Transbrasiliano Lineament (TBL)	Schobbenhaus et al. (2004)
9	Pirineus Syntaxis (PS)	Araújo Filho (2000)
10a	**Moiporá-Fazenda Nova Shear Zone (MFNSZ)**	Adapted from Araújo (2012); Macedo et al. (2018); Pimentel and Fuck (1992)
10b	**Messianópolis-Novo Brasil Shear Zone (MNBSZ)**	
11	Azimuth 125	Bardet (1977); Rocha et al. (2014, 2019a, 2019b)
12	Rio dos Bois Fault (RBF)	Fuck et al. (2014)
13	Rio Maranhão Fault (RMF)	
14	**São Luís dos Montes Belos-Ceres Shear Zone (SLMBSZ)**	Adapted from Araújo (2012); Macedo et al. (2018)
15	Anicuns Palmeiras Lineament (APL)	Lacerda Filho et al. (2018)
16	**Adelândia-Moquém Lineament (AML)**	
17	**Itapuranga-Bela Vista de Goiás Lineament (IBVL)**	
18	**Heitoraí-Araguaçu Lineament (HAL)**	
19	**Guaraíta-Palmeirópolis Lineament (GPL)**	
20	**Ceres-Minaçu Lineament (CML)**	
21	**Aragarças-Jesúpolis Lineament (AJL)**	
22	**Nova Xavantina-Moquém Lineament (NXML)**	
23	**Fazenda Nova-Aragoiânia Lineament (FNAL)**	
24	**Guaraíta-Mimoso de Goiás Lineament (GMGL)**	
25	**Matrinchã-Ouro Verde de Goiás Lineament (MOVGL)**	
26	**Piranhas-Amorinópolis Lineament (PAL)**	**This study**
27	**Uirapuru-Porangatu Lineament (UPL)**	
28	**Nova Xavantina-Novo Planalto Lineament (NXNPL)**	
29	**Itapaci-Santa Terezinha de Goiás Lineament (ISTL)**	
30	**Uirapuru-Niquelândia Lineament (UNL)**	
31	**Porangatu-Minaçu Lineament (PML)**	
32	**Mutunópolis-Campinaçu Lineament (MCL)**	
36	**Piranhas-Jussara Lineament (PJL)**	
44	**Paraúna-Inhumas Lineament (PIL)**	
46	**Uruana-Araguaiana Lineament (UAL)**	
50	**Guarino-Barro Alto Lineament (GBAL)**	

in the GMA, indicating thinner lithosphere under AMA-W, about 150 km, and a possible relationship with the Trindade Plume. The lithosphere thickness increases to the east of the X-X' profile modeled, reaching about 175 km (Assumpçao et al., 2002; Rocha et al., 2011, 2016, 2019a, 2019b; Gibson et al., 1995, 1997, 1999). We believe that the AMA-W thinner lithosphere may have facilitated the partial melting of the mantle and generation of the GAP due to the impact of the Trindade Plume in the Mesozoic.

The AMA-E is approximately 125 km long extending to the APL (15) vicinity to the east, and representing, in-depth, the suture between AMA-E and SFPC (Fig. 11). Geochemical and geochronological data from the Anicuns (Goiás state) suggest that the Araxá/Andrelândia Groups (Fig. 2) represent a fore-arc sequence and mark the tectonic boundary between the GMA eastern edge and the SFPC (Laux et al., 2005, 2010). In the magnetic data, the same magnetic arc response was observed in the region to the east of APL (15) and south of the MOVGL (25), to the vicinity of Goiânia (Goiás state) and Edéia (Goiás state) (Fig. 8). However, the geological data marks the GMA continuity, following only towards Edéia (Pimentel, 2016). The arc eastern boundary, in this portion of the study area, was inconclusive in our modeling, and additional work is needed to verify whether this portion south and southeastern edge of the GMA, is part of the AMA-E or if there is another magmatic arc separated by the APL.

The AMA-E boundary with the southern portion of the GM occurs through the MOVGL (25), MNBSZ (10b) (Pimentel et al., 1996) and HAL (18) (Fig. 13). We believe that the NE limit, south of Ceres (Goiás state) is marked by the MOVGL (25) since, to the north of this structure the PJL (36) and lineaments (37), (49) and (53), occurring in AMA-W and AMA-E are not observed, just like HAL (18) does not occur in GMA (Fig. 12D), being bounded by MOVGL (25).

Magnetic anomalies and lineaments north of MOVGL (25) have a different pattern from that observed in AMA-E (Figs. 8 and 9), which continues towards the south, covered by the Paraná Basin, and the magnetic, gravity and crustal thickness characteristics representing the Geophysical Domain 6 identified by Pinto and Vidotti (2019). The AMA-E has intermediate magnetic (Fig. 5) and gravity anomalies (Fig. 7), crustal thickness of 34 km, less than the AMA-W, and Currie depth between 43 km and 48 km (Rocha et al., 2019a, 2019b), in agreement with the lower crustal thickness of the block (Assumpção et al., 2013; Bernardes, 2015; Pavão, 2014). The lithosphere thickness varies about 150−160 km (Rocha et al., 2019a, 2019b) and the anomalies of S and P waves have high speed, characteristic of a cooler lithosphere (Rocha et al., 2011, 2016, 2019a, 2019b), unlike that observed in GMA and AMA-W. These features allowed us to interpret that the lithosphere under the AMA-E may have been altered during the collision with the SFPC.

The Arenópolis Magmatic Arc was formed by two accretion events between 821 Ma to 782 Ma (Laux et al., 2005) and was responsible for forming the AMA-W. Whereas the second accretion event that formed AMA-E, took place between 669 Ma to 639 Ma, and generated rocks with an Nd isotopic signature indicating ancient sialic material, confirming the SFPC proximity or participation (Laux et al., 2005; Rodrigues et al., 1999).

Our geological model (Fig. 11) shows that in the collision with the SFPC, part of the AMA-E was raised and possibly delamination of the arc root was exhumed, being represented by the AIC. The exhumation of high-grade metamorphic rocks has also been reported in other parts of the Tocantins Province (Della Giustina et al., 2009a, 2009b; Gorayeb et al., 2017). The development of thrust systems with a vergence towards the São Francisco craton may have caused the exhumation of part of the root of the AMA-E (D'el-Rey Silva et al., 2008; Moreira et al., 2008), exposing the AIC, which is formed by high-grade metamorphic rocks, dating from the Neoproterozoic (Fischel et al., 1998; Piuzana et al., 2003a, 2003b, Pimentel et al., 1999).

High grade metamorphic rocks are formed by collisional orogeny (Zhang et al., 2018), examples of these exposure are

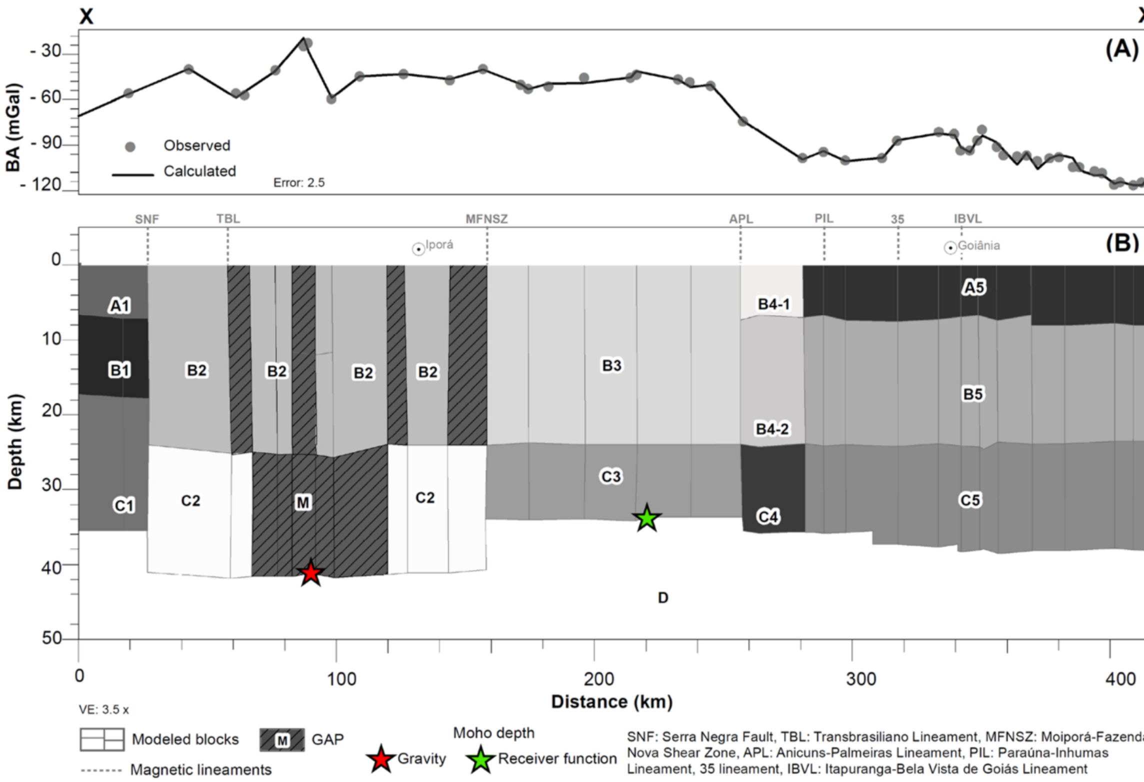

Fig. 10. Bouguer Anomaly profile showing observed anomaly (grey circle) and calculated anomaly (black line) (A). Geophysical model X-X' with modeled block (B), for details of the blocks see Table 3. Moho depth from gravity and receiver fuction are according to Assumpção et al. (2013); Bernardes (2015) and Pavão (2014). VE: vertical exaggeration.

Table 3
Physical and geological parameters of forward gravity modeling.

Lithospheric Domain	Block	Geological Unit	Associate Rock [a]	Density (kg/m^3) [b]		
				Min	Max	Mean
Upper Crust	A1	PB + PC	metasedimentary, granite	2663.8	2823.4	2743.6
	A5	AAG + AIC	quartzite, schist, paragneiss, marble, granulite	2664.8	2856.6	2769.6
	B2	AMA-W	calc alkaline orthogneiss, granite, volcanosedimentary	2975.6	2899.5.0	2858.3
	M	GAP [c]	dunite, pyroxenite, peridotite, nepheline syenite, alkaligrabbro, melanephelinite, olivine analcimite, basanite, etc.	2914.1	2996.9	2946.3
	B3	AMA-E	calc alkaline orthogneiss, granite, volcanosedimentary	2787.6	2812.4	2804.1
	B4−1	AMA-E				2753.8
	B1	GMA	orthogneiss, supracrustal	2708.3	2827.1	2767.7
	B4−2	SFPC	granodiorite, diorite			2683.5
	B5	SFPC		2611.5	2770.6	2716.4
Lower Crust [d]	M	GAP	dunite, pyroxenite, peridotite, nepheline syenite, alkaligrabbro, melanephelinite, olivine analcimite, basanite, etc.	2915.3	2945.8	2926.5
	C1	GMA	gabbro, mafic-ultramafic	2909.2	2937.4	2923.3
	C2	AMA-W		2860.9	2892.5	2867.5
	C3	AMA-E		2876.0	2981.4	2920.7
	C4	SFPC				2876.9
	C5	SFPC		2852.0	2962.1	2903
Mantle [d]	D		harzburgite, lherzolite			3368

PB: Paraguay Belt, PC: Phanerozoic Cover, AAG: Araxá/Andrelândia Groups, AIC: Anápolis Itauçu Complex, AMA: Arenópolis Magmatic Arc (W: West, E: East), GAP: Goiás Alkaline Province, GMA: Goiás Magmatic Arc, SFPC: São Francisco Paleocontinent.
[a] Alvarenga and Trompette (1993); Fuck et al. (2014); Pimentel et al. (2000a, 2000b, 2004); Pimentel (2016).
[b] Telford et al. (1990).
[c] Brod et al. (2005).
[d] Kearey et al. (2009).

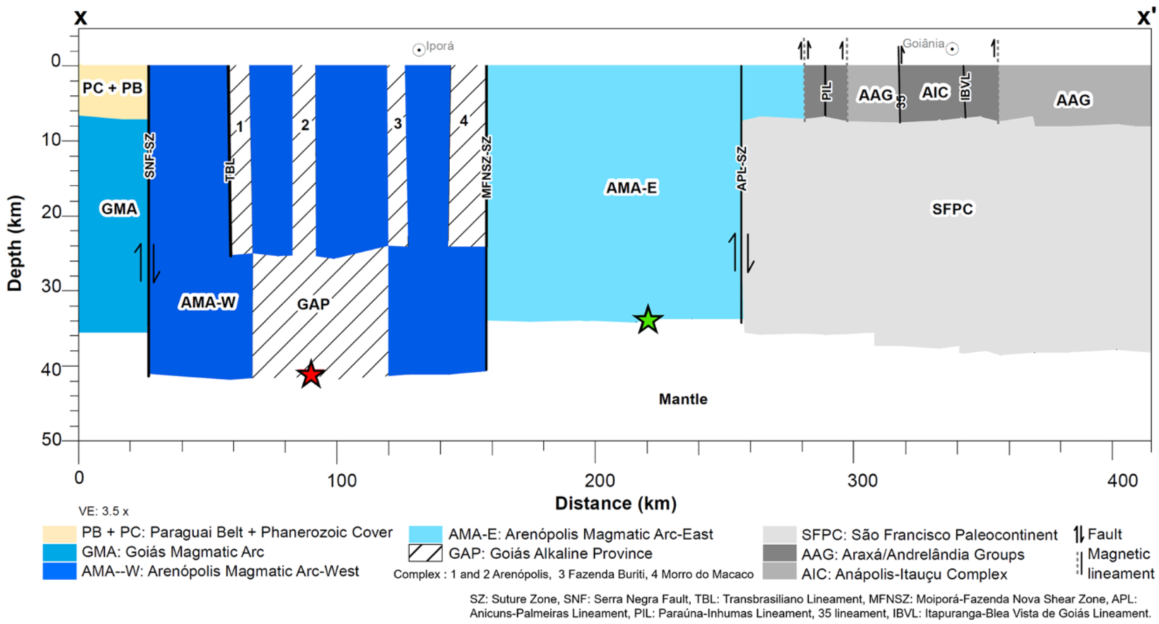

Fig. 11. Geological model based on 2.5 D geophysical model (Fig. 10B) and geological data. VE: vertical exaggeration.

Anápolis-Itauçu-Complex (AIC), in the study area (Moraes et al., 2002, 2007; Piuzana et al., 2003a, 2003b), Altun-Qilian-North Qaidam, NW China orogenc system (Zhang et a., 2018) and the Dabie-Sulu orogenic belt, NE China (Zheng et al., 2020). It indicate metamorphism between 100–150 km depth and surface exposure represents an extreme case of exhumation of root orogen (Ring et al., 1999), that can occur in the early stages of a continental subduction or may be related to a continental collision (Teyssier, 2011). The collisional orogeny evolves from a sin collisional phase with crustal shortening to a post collisional phase with crustal thinning. This transtition is marked by transtensional strucutres formation, such as ductile shear zones, wich can be subject to the exhumation of high grade metamorphic rocks, as reported in Altun-Qilian-North Qaidam orogenic system (Zhang et al., 2018). Structures like these may have been responsible for the exhumation of the AIC (Moraes et al., 2002, 2007) wich has as protoliths the Goiáas Magmatic Arc Neoproterozoic rocks (Piuzana et al., 2003a, 2003b).

There are still many doubts about the origin of the AIC, however, it is known that it does not represent the exposure of an Archean sialic basement as stated by Lacerda Filho et al. (1999). The replacement of the lithospheric mantle by the asthenospheric one, and the displacement of the orogenic root or the slab break-off may have been the possible mechanisms responsible for forming the AIC (Moraes et al., 2002).

During the collision of the Arenópolis Magmatic Arc (AMA) whit the São Francisco Paleocontinente (SFPC) part of the lithosphere of the Arenópolis Magmatic Arc-East (AMA-E) may have been removed by convective forces and exhumed to the surface. The exhumed rocks, AIC, occur interlayed with the Anapolis-Itauçu complex (Fig. 11). After exhumation the AMA lithospheric mantle may have been replaced by astenospheric mantle and this change in mantelic characteristics affected only the AMA-E wich is closer to SFPC (Laux et al., 2005; Rodrigues et al., 1999). We believe that the exhumation process changed the original characteristics of the primitive mantle over AMA-E, not allowing the formation of alkaline provinces.

5. Conclusions

The geophysical data analysis revealed the tectonic structures of the Tocantins Province, one of the most complete Neoproterozoic (Brasiliano – Pan African) Orogen in Western Gondwana, and their relationship with Goiás Alkaline Province.

We interpret the continuity of large tectonic structures in-depth, up to approximately 20 km, such as Rio Maranhão Fault, Baliza-Hidrolina Fault and Guaraíta-Palmeirópolis Lineament.

The GMA was divided into GMA, AMA-W and AMA-E crustal blocks, delimited by Serra Negra Fault, Moiporá-Fazenda Nova Shear Zone and Anicuns Palmeiras Lineament.

The GMA has a smaller crustal thickness than AMA-W, concentrates a large part of the earthquakes and is bounded by the Baliza-Hidrolina Fault to the east and by General Carneiro Fault to the west.

The AMA-W is bounded by the Baliza-Hidrolina Fault and Lineament 34 to the north, Serra Negra Fault to the west, Moiporá-Fazenda Nova Shear Zone to the east, and by the geophysical domains 4 and 5 to the south-southeast (Pinto and Vidotti, 2019). GAP occurs only in AMA-W that has the more primitive mantle and has not changed due to collision processes with the adjacent blocks, allowing the formation of alkaline rocks. In the AMA-W block the modeled section intercepted Arenópolis, Fazenda Buriti and Morro do Macaco complex, indicating a possible common magmatic source for the alkaline complexes located in the lower crust of this block.

The emplacement of the GAP occurred during the Gondwana breakup, preferably in the vicinity of NW-SE and NE-SW structures, generated at the end of Brasiliano orogeny and Mesozoic structures. From our analysis the GAP were not preferably concentrated along the Azimuth 125 trend. We believe that the Gondwana breakup possibly created and/or reactivated the structures related to Goiás Alkaline Province.

Locally the Azimuth 125 is displaced from the NW to the SE direction by the Moiporá-Fazenda Nova Shear Zone, Heitorai-Araguaçu Lineament and Rio Maranhão Fault. Moiporá-Fazenda Nova Shear Zone does not extend up to the LTB since it is limited by the Baliza-Hidrolina Fault to the north.

AMA-E is bounded by the Matrinchã-Ouro Verde de Goiás Lineament to the northeast, by the Anicuns Palmeiras Lineament to the east, and continues under the Paraná Basin to the south. This arc mantle has anomalous characteristics due to collision with the São Francisco Paleocontinent that avoid the formation of alkaline provinces.

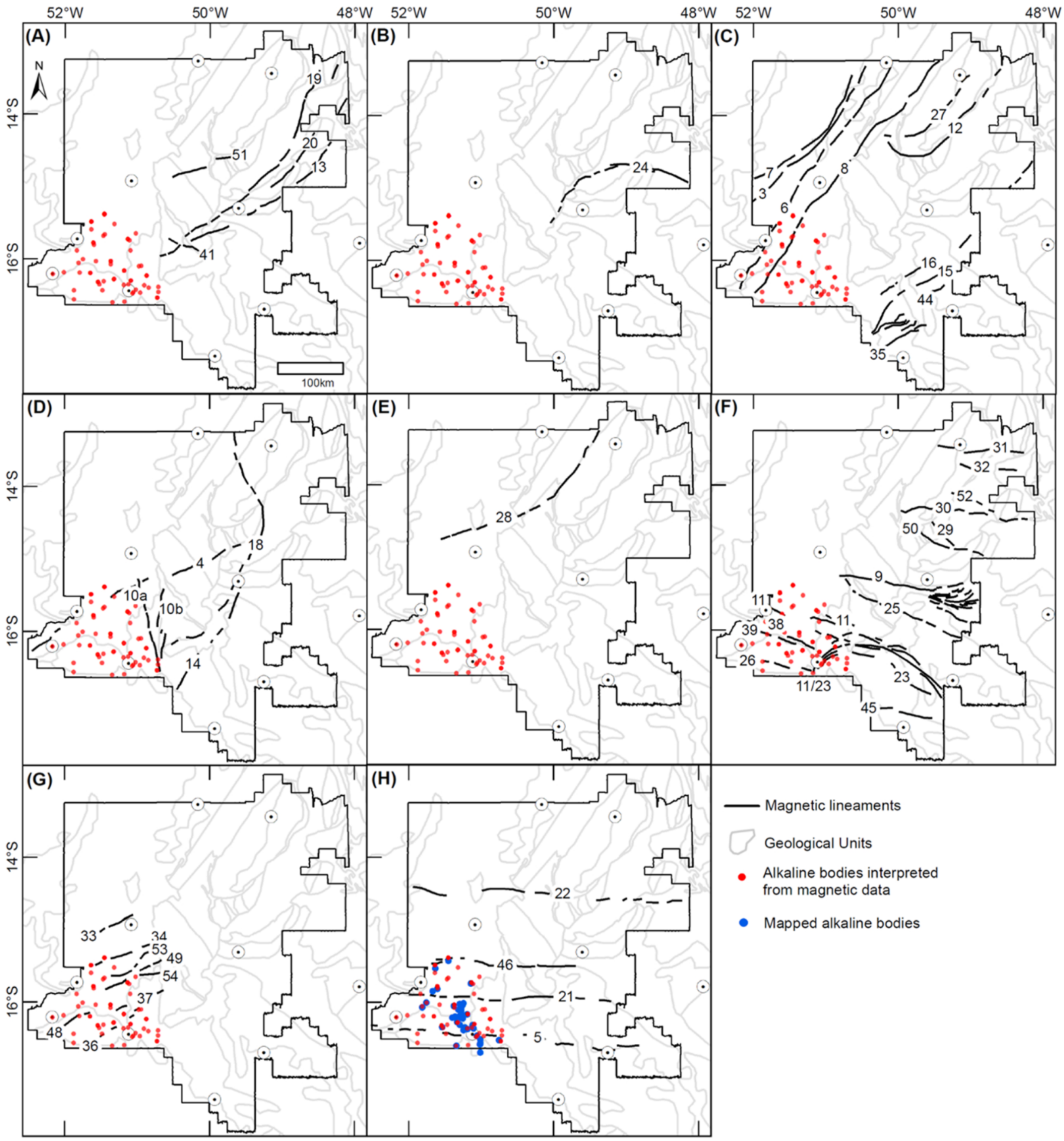

Fig. 12. Major magnetic lineaments associated with the evolution of the Tocantins Province (A, B: Archean/Paleoproterozoic age. C, D, E: Neoproterozoic age. F: Neoproterozoic to early Phanerozoic age. G: Mesozoic age. H: Cenozoic age). Blue circles represent mapped alkaline bodies (Lacerda Filho et al., 2018), Geological Units limits (according to Fig. 2) and magnetic lineament numbers (according to Table 2) (For interpretation of the references to colour in this figure legend, the reader is referred to the web version of this article.).

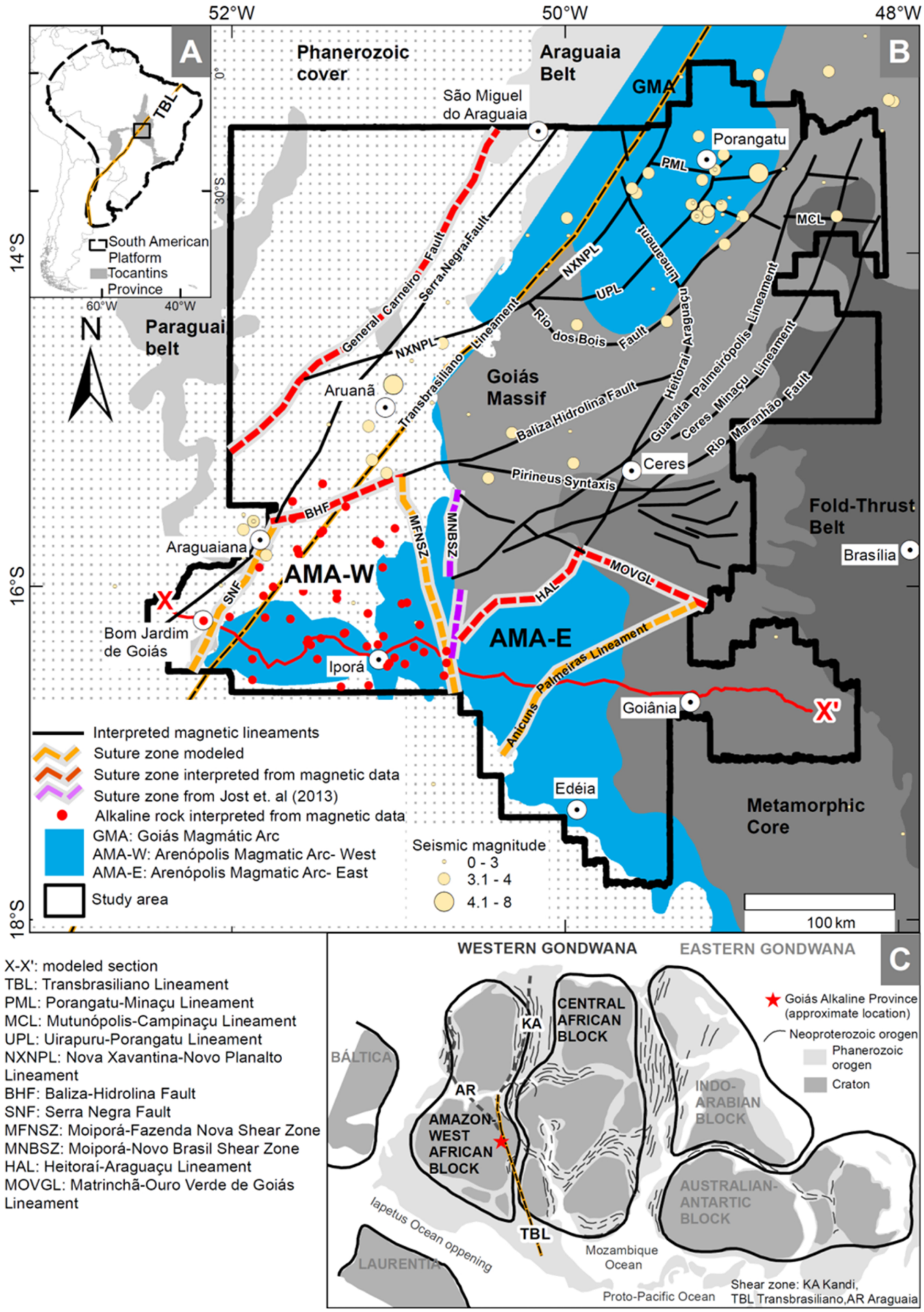

Fig. 13. Geophysical compartmentation of the Goiás Magmatic Arc. Seismic magnitude according to Assumpção et al. (2004, 2013); Cordani et al. (2013); Rocha et al. (2011, 2016); Soares et al. (2006).

The forward gravity modeling highlights a thick crust and a relative thin mantle (Rocha et al., 2019a, 2019b) below the AMA-W. We believe that the primitive mantle lithospheric in this block was not altered during the Brasiliano orogen stages like the adjacent crustal blocks allowing the generation of alkaline rocks.

Finaly, the geophysical data processing proved to be another way to study tectonic structures and alkaline provinces.

CRediT authorship contribution statement

Elainy S.F. Martins: Formal analysis, Conceptualization, Methodology, Writing - original draft, Writing - review & editing. **Roberta M. Vidotti:** Conceptualization, Methodology, Writing - review & editing.

Declaration of Competing Interest

The authors declare that they have no known competing financial interests or personal relationships that could have appeared to influence the work reported in this paper.

Acknowledgments

This study was financed in part by the Coordenação de Aperfeiçoamento de Pessoal de Nível Superior - Brazil (CAPES) - Finance Code 001. The authors are grateful to the Geological Survey of Brazil (CPRM) and Gravity National Bank (BNDG) for providing the aeromagnetic and gravity data used in this work. We also thank the Institute of Geosciences of the University of Brasilia (IG/UnB) for providing the infrastructure. We are particularly grateful to Dr. Claudinei Gouveia de Oliveira, Dr. Elton Luiz Dantas, and Dr. Elder Yokoyama for their suggestions on the occasion of the first author PhD Qualifying, and Marcelo Lima Pinto and Italo Lopes de Oliveira for the discussions on alkaline provinces and geophysical modeling. RMV is thankful to CNPq (Conselho Nacional de Desenvolvimento Científico e Tecnológico) for the grant provided (process 304739/2018-9). ESFM is thankful to UFOB (Universidade Federal do Oeste da Bahia) for grant leave of the lecturer for PhD qualification, also to Capes Dinter Project (code 1969/2016). We also thank two anonymous reviewers who made suggestions that improved our work. High resolution magnetic data used in this research paper is public domain data available from Geological Survey of Brazil (http://geosgb.cprm.gov.br/), Ground gravity data used in this work is public domain data, available under request (http://www.anp.gov.br/exploracao-e-producao-de-oleo-e-gas/dados-tecnicos/padroes-tecnicos-para-envio-de-dados-a-anp/bndg-banco-nacional-de-dados-gravimetricos) through the Banco Nacional de Dados Gravimétricos.

References

Alexandrino, C.H., Hamza, V.M., 2007. Estimates of heat flow and heat production and a thermal model of the São Francisco craton. Int. J. Earth Sci. 97 (2), 289–306. https://doi.org/10.1007/s00531-007-0291-y.

Almeida, F.F.M., 1966. Origem e evolução da plataforma brasileira. Sedegeo, Dv. Geol. Miner. 2, 46–89.

Almeida, F.F.M., 1971. Geochronological division of the precambrian of South America. Revista Brasileira de Geociências 1 (1), 13–21.

Almeida, F.F.M., 1983. Relações tectônicas das rochas alcalinas Mesozoicas da região meridional da Plataforma Sul-Americana. Revista Brasileira de Geociências 13 (3), 139–158.

Almeida, F.F.M., 1986. Distribuição regional e relações tectônicas do magmatismo pós-paleozoico no Brasil. Revista Brasileira de Geociências 16 (4), 325–349.

Almeida, F.F.M., Hasui, Y., Brito Neves, B.B., Fuck, R.A., 1981. Brazilian structural provinces: an introduction. Earth-Sci. Rev. 17 (1–2), 1–29. https://doi.org/10.1016/0012-8252(81)90003-9.

Almeida, F.F.M., Brito Neves, B.B., Carneiro, C.D.R., 2000. The origin and evolution of the South American Platform. Earth-Sci. Rev. 50 (1–2), 77–111. https://doi.org/10.1016/S0012-8252(99)00072-0.

Alvarenga, C.J., Trompette, R., 1993. Evolução tectônica brasiliana da Faixa Paraguai: a estruturação da região de Cuiabá. Revista Brasileira de Geociências 23 (1), 18–30.

Araújo, J.G.M., 2012. Eventos Ígneos e metamórficos Neoproterozoicos/Eo-paleozoicos no Arco Magmático de Arenópolis, Goiás. ix, 73 f., il. Tese (Doutorado em Geologia) - Universidade de Brasília, Brasília. https://repositorio.unb.br/handle/10482/16945.

Araújo Filho, J.O., 2000. The Pirineus Syntaxis: an example of the intersection of two Brasiliano fold-thrust belts in central Brazil and its implications for the tectonic evolution of western Gondwana. Revista Brasileira de Geociências 30 (1), 144–148.

Araújo Filho, J.O., Kuyumjian, R.M., 1996. Regional distribution and structural control of the gold occurrences/deposits in the Goiás Massif and Brasília Belt. Revista Brasileira de Geociências 26 (2), 109–112.

Assumpçao, M., James, D., Snoke, A., 2002. Crustal thicknesses in SE Brazilian Shield by receiver function analysis: implications for isostatic compensation. J. Geophys. Res. Solid Earth 107 (B1). https://doi.org/10.1029/2001JB000422. ESE-2-14.

Assumpção, M., An, M., Bianchi, M., França, G.S.L., Rocha, M., Barbosa, J.R., Berrocal, J., 2004. Seismic studies of the Brasília fold belt at the western border of the São Francisco Craton, Central Brazil, using receiver function, surface-wave dispersion and teleseismic tomography. Tectonophysics 388 (1-4), 173–185. https://doi.org/10.1016/j.tecto.2004.04.029.

Assumpção, M., Bianchi, M., Julià, J., Dias, F.L., França, G.S., Nascimento, R., Drouet, S., Pavão, C.G., Albuquerque, D.F., Lopes, A.E., 2013. Crustal thickness map of Brazil: data compilation and main features. J. South Am. Earth Sci. 43, 74–85. https://doi.org/10.1016/j.jsames.2012.12.009.

Azevedo, P.A., Rocha, M.P., Soares, J.E.P., Fuck, R.A., 2015. Thin lithosphere between the Amazonian and São Francisco cratons, in central Brazil, revealed by seismic P-wave tomography. Geophys. J. Int. 201 (1), 61–69. https://doi.org/10.1093/gji/ggv003.

Baranov, V., 1957. A new method for interpretation of aeromagnetic maps: pseudogravimetric anomalies. Geophysics 22 (2), 359–382. https://doi.org/10.1190/1.1438369.

Baranov, V., Naudy, H., 1964. Numerical calculation of the formula of reduction to the magnetic pole. Geophysics 29 (1), 67–79. https://doi.org/10.1190/1.1439334.

Bardet, M.G., 1977. Geólogie du diamante. Troisième partie: Gisementes de diamants d'Asie, d'Amérique, d'Europeet d'Australasie. Mémoires du Bur. Res. Geol. Min. 83, 169.

Bernardes, R.B., 2015. Modelo de Velocidade Sismica de Ondas P da Crosta e Manto Superior ao Longo do Perfil PABBRISE, Estado de São Paulo. M. Sc. Thesis. Instituto de Geociências, Universidade de Brasília, Brasília, Brazil, p. 92. https://repositorio.unb.br/handle/10482/20299.

Berrocal, J., Marangoni, Y., de Sá, N.C., Fuck, R., Soares, J.E., Dantas, E., Perosi, F., Fernandes, C., 2004. Deep seismic refraction and gravity crustal model and tectonic deformation in Tocantins Province, Central Brazil. Tectonophysics 388 (1-4), 187–199. https://doi.org/10.1016/j.tecto.2004.04.033.

Biondi, J.C., 2005. Brazilian Mineral Deposits Associated With Alkaline and Alkaline-Carbonatite Complexes. Mesozoic to Cenozoic alkaline magmatism in the Brazilian Platform, Edusp/Fapesp, São Paulo, pp. 707–750.

Bizzi, L.A., Araújo, A.L.N., 2005. Dynamics of Mantle Derived Magmatism in the Southwestern São Francisco Craton, Brazil. Mesozoic to Cenozoic alkaline magmatism in the Brazilian Platform. Edusp/Fapesp, São Paulo, pp. 341–365.

Bizzi, L.A., Schobbenhaus, C., Vidotti, R.M., Gonçalves, J.H., 2003. Geologia, Tectônica e Recursos Minerais do Brasil: texto, mapas e SIG. CPRM.

Blakely, R.J., 1996. Potential Theory in Gravity and Magnetic Applications. Cambridge University Press, United Kingdom, p. 441.

Brito Neves, B.B., Cordani, U.G., 1991. Tectonic evolution of South America during the late Proterozoic. Precambrian Res. 53 (1–2), 23–40.

Brito Neves, B.B., Fuck, R.A., 2013. Neoproterozoic evolution of the basement of the South-American platform. J. South Am. Earth Sci. 47, 72–89. https://doi.org/10.1016/j.jsames.2013.04.005.

Brito Neves, B.B.D., Fuck, R.A., Pimentel, M.M., 2014. The Brasiliano collage in South America: a review. Braz. J. Geol. 44 (3), 493–518. https://doi.org/10.5327/Z2317-4889201400030010.

Brod, J.A., Barbosa, E.S.R., Junqueira-Brod, T.C., Gaspar, J.C., Diniz-Pinto, H.S., Sgarbi, P.B.A., Petrinovic, I.A., 2005. The Late-Cretaceous Goiás Alkaline Province (GAP), Central Brazil. Mesozoic to Cenozoic Alkaline Magmatism in the Brazilian Plataform. Edusp/Fapesp, pp. 261–316.

Burke, K., Roberts, D., Ashwal, L.D., 2007. Alkaline rocks and carbonatites of northwestern Russia and northern Norway: linked Wilson cycle records extending over two billion years. Tectonics 26 (4). https://doi.org/10.1029/2006TC002052.

Cernuschi, F., Dilles, J.H., Kent, A.J.R., Schroer, G., Raab, A.K., Conti, B., Muzio, R., 2015. Geology, geochemistry and geochronology of the Cretaceous Lascano East Intrusive Complex and magmatic evolution of the Laguna Merín Basin, Uruguay. Gondwana Res. 28 (2), 837–857. https://doi.org/10.1016/j.gr.2014.07.007.

Comin-Chaiaramoti, P., Gomes, C., Cundari, A., Castorina, F., Censi, P., 2007. A review of carbonatitic magmatism in the Paraná-Angola-Namibia (PAN) system. Periodico di Mineralogia 76 (2-3), 25–78. https://doi.org/10.2451/2007PM0016.

Comin-Chiaramonti, P., Cundari, A., DeGraff, J.M., Gomes, C.B., Piccirillo, E.M., 1999. Early Cretaceous–tertiary magmatism in eastern Paraguay (Western Paraná Basin): geological, geophysical and geochemical relationships. J. Geodyn. 28 (4–5), 375–391. https://doi.org/10.1016/S0264-3707(99)00016-2.

Comin-Chiaramonti, P., Gomes, C.B., Velazquez, V.F., Censi, P., Antonini, P., Comin-Chiaramonti, F., Punturo, R., 2005. Alkaline Complexes From Southeastern Bolivia. Mesozoic to Cenozoic Alkaline Magmatism in the Brazilian Platform. Edusp-Fapesp, São Paulo, Brazil, pp. 159–212.

Comin-Chiaramonti, P., Gomes, C.B (Eds.), 1996. Alkaline Magmatism in Central-Eastern Paraguay: Relationships With Coeval Magmatism in Brazil. Edusp.

Cordani, U.G., Pimentel, M.M., Araújo, C.E.G., Fuck, R.A., 2013. The significance of the Transbrasiliano-Kandi tectonic corridor for the amalgamation of West Gondwana. Braz. J. Geol. 43 (3), 583–597. https://doi.org/10.5327/Z2317-48892013000300012.

Cordani, U.G., Ramos, V.A., Fraga, L.M., Cegarra, M., Delgado, I., Souza, K.G.D., Gomes, F.E.M., Schobbenhaus, C., 2016. Tectonic Map of South America - Mapa

tectônico da América do Sul, 2nd. ed. CGMW-CPRM-SEGEMAR, Paris. 1 map. Scale 1:5.000.000.
Cordeiro, P.F.O., Oliveira, C.G., 2017. The Goiás Massif: implications for a pre-Columbia 2.2–2.0 Ga continent-wide amalgamation cycle in central Brazil. Precambrian Res. 298, 403–420. https://doi.org/10.1016/j.precamres.2017.06.021.
Cordeiro, P.F.O., Oliveira, C.G., Giustina, M.E.S.D., Dantas, E.L., dos Santos, R.V., 2014. The paleoproterozoic campinorte arc: tectonic evolution of a central Brazil pre-columbia orogeny. Precambrian Res. 251, 49–61. https://doi.org/10.1016/j.precamres.2014.06.002.
Cordell, L., Grauch, V.J.S., 1985. Mapping basement magnetization zone from aeromagnetic data in the San Juan basin Mexico. In: Hinze, W.M. (Ed.), The Utility of Regional Gravity and Magnetic Anomaly Maps Vol. 16, 181–197. https://doi.org/10.1190/1.0931830346.ch16.
Cowan, D.R., Cowan, S., 1993. Separation filtering applied to aeromagnetic data. Explor. Geophys. 24 (3-4), 429–436. https://doi.org/10.1071/EG993429.
CPRM, 1974. Projeto Iporá: Relatório de Aerogamaespectrometria e Aeromagnetometria na Área do Projeto Iporá, nos Estados de Goiás e Mato Grosso. CPRM, Rio de Janeiro.
CPRM, 2004a. SERVIÇO GEOLÓGICO DO BRASIL. Levantamento aerogeofísico do estado de Goiás - 1ª etapa: arco magmático de Mara Rosa: relatório final do levantamento e processamento dos dados magnetométricos e gamaespectrométricos. Lasa Engenharia e Prospecções, Rio de Janeiro, 12 v.
CPRM, 2004b. SERVIÇO GEOLÓGICO DO BRASIL. Levantamento aerogeofísico do estado de Goiás - 1ª etapa: arco magmático de Arenópolis: relatório final do levantamento e processamento dos dados magnetométricos e gamaespectrométricos. Lasa Engenharia e Prospecções, Rio de Janeiro.
CPRM, 2005. SERVIÇO GEOLÓGICO DO BRASIL. Levantamento aerogeofísico do estado de Goiás - 2ª etapa: oeste do arco magmático de Mara Rosa: relatório final do levantamento e processamento dos dados magnetométricos e gamaespectrométricos. Lasa Engenharia e Prospecções, Rio de Janeiro, 7 v.
CPRM, 2012. SERVIÇO GEOLÓGICO DO BRASIL. Projeto Aerogeofísico Sudeste do Mato Grosso: relatório final do levantamento e processamento dos dados magnetométricos e gamaespectrométricos. Lasa Prospecções. Programa Geologia do Brasil (PGB), Rio de Janeiro.
Curto, J.B., Vidotti, R.M., Fuck, R.A., Blakely, R.J., Alvarenga, C.J.S., Dantas, E.L., 2014. The tectonic evolution of the Transbrasiliano Lineament in northern Parana Basin, Brazil, as inferred from aeromagnetic data. J. Geophys. Res. Solid Earth 119 (3), 1544–1562. https://doi.org/10.1002/2013JB010593.
Curto, J.B., Vidotti, R.M., Blakely, R.J., Fuck, R.A., 2015. Crustal framework of the northwest Parana Basin, Brazil: insights from joint modeling of magnetic and gravity data. Tectonophysics 655, 58–72. https://doi.org/10.1016/j.tecto.2015.05.011.
D'el-Rey Silva, J.H., Vasconcelos, M.A.R., Silva, D.V.G., 2008. Timing and role of theMaranhão river thrust in the evolution of the neoproterozoic Brasília Belt and Tocantins Province, central Brazil. Gondwana Res. 13, 352–374. https://doi.org/10.1016/j.gr.2007.09.004.
Danni, J.C., 1994. Os picritos alcalinos da região de Iporá: implicações na gênese dos complexos do tipo central do Sul de Goiás. Revista Brasileira de Geociências 24 (2), 112–119.
Danni, J.C.M., Gaspar, J.C., 1994. Química do katungito de Amorinópolis-Goiás: contribuição ao estudo do magmatismo kamafugítico. Geochim. Bras. 8, 119–134. https://doi.org/10.21715/gb.v8i2.73.
Danni, J.C.M., Silva, A.J., Cerqueira, M.R., 1990. Petrografia e petroquímica das rochas alcalinas cretácicas da Serra do Caiapó, SW de Goiás. CONGR. BRÁS. GEOL., 36. Natal, 1990. Anais… Natal, SBG 4, 1872–1882.
Della Giustina, M.E.S., Oliveira, C.G., Pimentel, M.M., Buhn, B., 2009a. Neoproterozoic magmatism and high-grade metamorphism in the Goiás Massif: new LA-MC-ICMPS U–Pb and Sm–Nd data and implications for collisional history of the Brasília Belt. Precambrian Res. 172 (1–2), 67–79. https://doi.org/10.1016/j.precamres.2009.03.012.
Della Giustina, M.E.S., Oliveira, C.G., Pimentel, M.M., Melo, L.V., Fuck, R.A., Dantas, E. L., Buhn, B., 2009b. U-Pb and Sm-Nd constraints on the nature of the Campinorte sequence and related Palaeoproterozoic juvenile orthogneisses, Tocantins Province, central Brazil. Geol. Soc. London Spec. Publ. 323 (1), 255–269. https://doi.org/10.1144/SP323.12.
Dutra, A.C., Marangoni, Y.R., 2009. Gravity and magnetic 3D inversion of Morro do Engenho complex, Central Brazil. J. South Am. Earth Sci. 28 (2), 193–203. https://doi.org/10.1016/j.jsames.2009.02.006.
Dutra, A.C., Marangoni, Y.R., Junqueira-Brod, T.C., 2012. Investigation of the goiás alkaline province, Central Brazil: application of gravity and magnetic methods. J. South Am. Earth Sci. 33 (1), 43–55. https://doi.org/10.1016/j.jsames.2011.06.004.
Dutra, A.C., Marangoni, Y.R., Trindade, R.I., 2014. Aeromagnetic and physical-chemical properties of some complexes from Goiás Alkaline Province. Braz. J. Geol. 44 (3), 361–373. https://doi.org/10.5327/Z2317-4889201400030003.
Feitoza, L.M., 2011. Assinatura geofísica das rochas alcalinas da porção norte da Província Alcalina de Goiás. ix, 182f., il. Dissertação (Mestrado em Geofísica Aplicada) - Universidade de Brasília, Instituto de Geociências. https://repositorio.unb.br/handle/10482/8971.
Ferreira, C.O., 2009. A extensão do arco magmático de Goiás ao longo do lineamento transbrasiliano: estudo baseado na aplicação dos métodos U-Pb e Lu-Hf por LA-MC-ICP-MS. 91 f. Dissertação (Mestrado em Geologia) - Universidade de Brasília, Brasília, Instituto de Geociências. https://repositori.unb.br/handle/10482/4204.
Ferreira, F.J., de Souza, J., Bongiolo, A.B.S., de Castro, L.G., 2013. Enhancement of the total horizontal gradient of magnetic anomalies using the tilt angle. Geophysics 78 (3), J33–J41. https://doi.org/10.1190/geo2011-0441.1.
Fischel, D.P., Pimentel, M.M., Fuck, R.A., 1998. Idade do metamorfismo de alto grau no Complexo Anápolis-Itauçu, Goiás, determinada pelo método Sm-Nd. Revista Brasileira de Geociências 28 (4), 543–544.
Fuck, R.A., Neves, B.B.B., Schobbenhaus, C., 2008. Rodinia descendants in south America. Precambrian Res. 160 (1–2), 108–126. https://doi.org/10.1016/j.precamres.2007.04.018.
Fuck, R.A., Dantas, E.L., Pimentel, M.M., Botelho, N.F., Armstrong, R., Laux, J.H., Junges, S.L., Amstrong, R., Soares, J.E.S., Praxedes, I.F., 2014. Paleoproterozoic crust-formation and reworking events in the Tocantins Province, central Brazil: a contribution for Atlantica supercontinent reconstruction. Precambrian Res. 244, 53–74. https://doi.org/10.1016/j.precamres.2013.12.003.
Fuck, R.A., Pimentel, M.M., Alvarenga, C.J., Dantas, E.L., 2017. The northern Brasília belt. São Francisco Craton, Eastern Brazil. Springer, Cham, pp. 205–220.
Gibson, S.A., Thompson, R.N., Leonardos, O.H., Dickin, A.P., Mitchell, J.G., 1995. The Late Cretaceous impact of the Trindade mantle plume: evidence from large-volume, mafic, potassic magmatism in SE Brazil. J. Petrol. 36 (1), 189–229. https://doi.org/10.1093/petrology/36.1.189.
Gibson, S.A., Thompson, R.N., Weska, R.K., Dickin, A.P., Leonardos, O.H., 1997. Late Cretaceous rift-related upwelling and melting of the Trindade starting mantle plume head beneath western Brazil. Contrib. Mineral. Petrol. 126 (3), 303–314. https://doi.org/10.1007/s004100050252.
Gibson, S.A., Thompson, R.N., Leonardos, O.H., Dickin, A.P., Mitchell, J.G., 1999. The limited extent of plume-lithosphere interactions during continental flood-basalt genesis: geochemical evidence from Cretaceous magmatism in southern Brazil. Contrib. Mineral. Petrol. 137 (1–2), 147–169. https://doi.org/10.1007/s004100050588.
Gomes, C.B., Ruperti, E., Morbidelli, L., 1990. Carbonatite complexes from Brazil: a review. J. South Am. Earth Sci. 3 (1), 51–63. https://doi.org/10.1016/0895-9811(90)90017-U.
Gomes, C.B., Comin-Chiaramonti, P., Azzone, R.G., Ruberti, E., Rojas, G.E.E., 2018. Cretaceous carbonatites of the southeastern Brazilian Platform: a review. Braz. J. Geol. 48 (2), 317–345. https://doi.org/10.1590/2317-4889201820170123.
Gorayeb, P.S.S., Pimentel, M.M., Armstrong, R., Galarza, M.A., 2017. Granulite-facies metamorphism at ca. 570-580 Ma in the Porangatu Granulite Complex, central Brazil: implications for the evolution of the Transbrasiliano Lineament. Braz. J. Geol. 47 (2), 327–344. https://doi.org/10.1590/2317-4889201720160097.
Grauch, V.J.S., Cordell, L., 1987. Limitations of determining density or magnetic boundaries from the horizontal gradient of gravity or pseudogravity. Geophysics 52 (1), 118–121. https://doi.org/10.1190/1.1442236.
Hamza, V.M., Dias, F.J.S., Gomes, A.J., Terceros, Z.G.D., 2005. Numerical and functional representations of regional heat flow in South America. Phys. Earth Planet. Inter. 152 (4), 223–256. https://doi.org/10.1016/j.pepi.2005.04.009.
Hamza, V., Vieira, F., Gomes, J., Guimaraes, S., Alexandrino, C., Gomes, A., 2020. Update of Brazilian Heat Flow Data, within the framework of a multiprong referencing system. International Journal of Terrestrial Heat Flow and Applied Geothermics 3 (1), 45–72. https://orcid.org/0000-0002-1143-0001.
Hasui, Y., 2010. A grande colisão pré-cambriana do sudeste brasileiro e a estruturação regional. Geociências 141–169.
Hinze, W.J., Von Frese, R.R.B., Saad, A.H., 2013. Gravity and Magnetic Exploration: Principles, Practices, and Applications. Cambridge University Press, United Kingdom, p. 502.
Isles, D.J., Rankin, L.R., 2013. Geological Interpretation of Aeromagnetic Data. The Australian Society of Exploration Geophysicists, Australia, p. 351.
Jacques, J.M., 2003a. A tectonostratigraphic synthesis of the Sub-Andean basins: implications for the geotectonic segmentation of the Andean Belt. J. Geol. Soc. 160 (5), 687–701. https://doi.org/10.1144/0016-764902-088.
Jacques, J.M., 2003b. A tectonostratigraphic synthesis of the Sub-Andean basins: inferences on the position of South American intraplate accommodation zones and their control on South Atlantic opening. J. Geol. Soc. 160 (5), 703–717. https://doi.org/10.1144/0016-764902-089.
Jacques, J.M., 2004. The influence of intraplate structural accommodation zones on delineating petroleum provinces of the Sub-Andean foreland basins. Pet. Geosci. 10 (1), 1–19. https://doi.org/10.1144/1354-079303-582.
Jost, H., Fuck, R.A., Dantas, E.L., Rancan, C.C., Rezende, D.B., Santos, E., Portela, J.F., Mattos, L., Chiarini, M.F.N., Oliveira, R.C., Silva, S.E., 2005. Geologia e geocronologia do Complexo Uvá, bloco arqueano de Goiás. Revista Brasileira de Geociências 35 (4), 559–572.
Jost, H., Junior, F.C., Fuck, R.A., Dussin, I.A., 2013. Uvá complex, the oldest orthogneisses of the Archean-Paleoproterozoic terrane of central Brazil. J. South Am. Earth Sci. 47, 201–212. https://doi.org/10.1016/j.jsames.2013.07.002.
Junqueira-Brod, T.C., Gaspar, J.C., Brod, J.A., Jost, H., Barbosa, E.S.R., Kafino, C.V., 2005a. Emplacement of kamafugite lavas from the Goiás alkaline province, Brazil: constraints from whole-rock simulations. J. South Am. Earth Sci. 18 (3–4), 323–335. https://doi.org/10.1016/j.jsames.2004.11.001.
Junqueira-Brod, T.C., Gaspar, J.C., Brod, J.A., Kafino, C.V., 2005b. Kamafugitic diatremes: their textures and field relationships with examples from the Goiás alkaline province, Brazil. J. South Am. Earth Sci. 18 (3–4), 337–353. https://doi.org/10.1016/j.jsames.2004.11.002.
Kearey, P., Klepeis, K.A., Vine, F.J., 2009. Global Tectonics, 3rd. John Wiley and Sons, p. 482.
Kirstein, L.A., Peate, D.W., Hawkesworth, C.J., Turner, S.P., Harris, C., Mantovani, M.S., 2000. Early Cretaceous basaltic and rhyolitic magmatism in southern Uruguay associated with the opening of the South Atlantic. J. Petrol. 41 (9), 1413–1438. https://doi.org/10.1093/petrology/41.9.1413.
Lacerda Filho, J.V.D., Rezende, A., Silva, A.D., 1999. Geologia e recursos minerais do Estado de Goiás e Distrito Federal: texto explicativo dos mapas geológico e de

recursos minerais do estado de Goiás e Distrito Federal. CPRM; METAGO; UNB, 1999. Programa Levantamentos Geológicos Básicos do Brasil – PLGB, Goiânia.
Lacerda Filho, J.V., Santos, D.R.V., Meneghini, P.F.V.B., Martins, F.R., Souza, J.O., Carneiro, J.S.M., Gollmann, K., 2018. Projeto oeste de Goiás: mapa geológico-geofísico integrado. CPRM, Goiânia. Escala 1:250.000. (Programa Novas Fronteiras: Levantamento Geológico e potencial de Novas Fronteiras).
Lagorio, S.L., 2008. Early Cretaceous alkaline volcanism of the Sierra Chica de Córdoba (Argentina): mineralogy, geochemistry and petrogenesis. J. South Am. Earth Sci. 26 (2), 152–171. https://doi.org/10.1016/j.jsames.2008.05.003.
Lasa, 2006. Engenharia e Prospecção S.A., "Projeto Levantamento Aerogeofísico do Estado de Goiás – 3a Etapa – Paleo-Neoproterozóico do nordeste de Goiás – Relatório final do levantamento e processamento dos dados magnetométricos e gamaespectrométricos", Convênio de cooperação entre a SGM/MME/CPRM e SIC/SGM/FUNMINERAL/ Estado de Goiás, Relatório Final, 22 vol., Texto e Anexos (mapas), Rio de Janeiro.
Laux, J.H., Pimentel, M.M., Dantas, E.L., Armstrong, R., Armele, A., Nilson, A.A., 2004. Mafic magmatism associated with the Goiás magmatic arc in the Anicuns region, Goiás, central Brazil: Sm–Nd isotopes and new ID-TIMS and SHIMP U–Pb data. J. South Am. Earth Sci. 16 (7), 599–614. https://doi.org/10.1016/j.jsames.2003.11.001.
Laux, J.H., Pimentel, M.M., Dantas, E.L., Armstrong, R., Junges, S.L., 2005. Two Neoproterozoic crustal accretion events in the Brasília belt, central Brazil. J. South Am. Earth Sci. 18 (2), 183–198. https://doi.org/10.1016/j.jsames.2004.09.003.
Laux, J.H., Pimentel, M.M., Gioia, S.M.C., Ferreira, V.P., 2010. The Anicuns-Itaberaí volcano-sedimentary sequence, Goiás Magmatic Arc: new geochemical and Nd-Sr isotopic data. Geochim. Bras. 24 (1), 13–28.
Lustrino, M., Melluso, L., Brotzu, P., Gomes, C.B., Morbidelli, L., Muzio, R., Excelcio, R., Tassinari, C.G.C., 2005. Petrogenesis of the early Cretaceous Valle Chico igneous complex (SE Uruguay): relationships with Paraná–etendeka magmatism. Lithos 82 (3), 407–434. https://doi.org/10.1016/j.lithos.2004.07.004.
Macedo, H.A.O., Della Giustina, M.E.S., de Oliveira, C.G., Praxedes, I.F., 2018. The São Luís de Montes Belos vermiculite deposit, central Brazil: Hydrothermal mineralization associated with intracontinental strike slip zones. J. South Am. Earth Sci. 88, 459–479. https://doi.org/10.1016/j.jsames.2018.08.012.
Mantovani, M.S.M., Louro, V.H.A., Ribeiro, V.B., Requejo, H.S., dos Santos, R.P.Z., 2015. Geophysical analysis of Catalão I alkaline–carbonatite complex in Goiás, Brazil. Geophys. Prospect. 64 (1), 216–227. https://doi.org/10.1111/1365-2478.12283.
Marangoni, Y.R., Mantovani, M.S., 2013. Geophysical signatures of the alkaline intrusions bordering the Paraná Basin. J. South Am. Earth Sci. 41, 83–98. https://doi.org/10.1016/j.jsames.2012.08.004.
Marangoni, Y.R., Zhang, H., Ferreira, H.J., 2015. Gravity and magnetic integrated data interpretation of the Córrego dos Bois complex, Goiás Alkaline Province, central Brazil. Braz. J. Geophys. 33 (4), 599–610. https://doi.org/10.22564/rbgf.v33i4.756.
Matton, G., Jébrak, M., 2009. The Cretaceous Peri-Atlantic Alkaline Pulse (PAAP): deep mantle plume origin or shallow lithospheric break-up? Tectonophysics 469 (1-4), 1–12. https://doi.org/10.1016/j.tecto.2009.01.001.
Miranda, R., Valadares, V., Terrinha, P., Mata, J., do Rosario Azevedo, M., Gaspar, M., Kullberg, J.C., Ribeiro, C., 2009. Age constraints on the late cretaceous alkaline magmatism on the west iberian margin. Cretac. Res. 30 (3), 575–586. https://doi.org/10.1016/j.cretres.2008.11.002.
Moraes, R., Brown, M., Fuck, R.A., Camargo, M.A., Lima, T.M., 2002. Characterization and P–T evolution of melt-bearing ultrahigh-temperature granulites: an example from the Anápolis–Itauçu Complex of the Brasília Fold Belt, Brazil. J. Petrol. 43 (9), 1673–1705. https://doi.org/10.1093/petrology/43.9.1673.
Moraes, R., Fuck, R.A., Brown, M., Piccol, P., Baldwin, J., Danta, E.L., Laux, J.H., Junge, S.L., 2007. Wollastonite–scapolite–clinopyroxene marble of the Anápolis-Itauçu Complex, Goiás: more evidence of ultrahigh-temperature metamorphism. Braz. J. Geol. 37 (4), 11–17.
Morbidelli, L., Gomes, C.B., Beccaluva, L., Brotzu, P., Conte, A.M., Ruberti, E., Traversa, G., 1995. Mineralogical, petrological and geochemical aspects of alkaline and alkaline-carbonatite associations from Brazil. Earth. Rev. 39 (3–4), 135–168. https://doi.org/10.1016/0012-8252(95)00031-3.
Moreira, M.L.O., Moreton, L.C., Araújo, V.A.D., Lacerda Filho, J.V.D., Costa, H.F.D., 2008. Geologia do estado de Goiás e Distrito Federal: texto explicativo do mapa geológico do estado de Goiás e Distrito Federal. CPRM; SIC - FUNMINERAL, Goiânia, 2008. Escala 1:500.000. Programa Geologia do Brasil (PGB); Programa Geologia e Mineração do Estado de Goiás.
Motta-Araújo, J.G., Pimentel, M.M., 2003. U-Pb ages, Sm-Nd isotopes and structural analysis of the Moipora-Novo brasil shear zone system: the limits between Neoproterozoic Goiás Magmatic Arc and the Archean Uvá Complex, Tocantins Province, central brazil. Symposium on Isotope Geology.
Ohofugi, W., Barreto Filho, J.A., Almeida, V.J., Vivian, O., Eulalio Filho, A., 1976. Projeto geofísico na área do Rio Caiapó: Relatório final. CPRM, Goiânia, 5 v.
Oliveira, C.G., Queiroz, C.L., Pimentel, M.M., 2000. The Arenopólis-Mara Rosa gold-copper belt, neoproterozoic goiás magmatic arc. Revista Brasileira de Geociências 30 (2), 219–221.
Oliveira Jr., V.C., Sales, D.P., Barbosa, V.C.F., Uieda, L., 2015. Estimation of the total magnetization direction of approximately spherical bodies. Nonlinear Process. Geophys. 22 (2), 215–232. https://doi.org/10.5194/npg-22-215-2015.
Pavão, C.G., 2014. Avaliação de Metodologias de Interpolação Espacial para Dados Geofísicos de Espessura Crustal do Brasil Ph. D. Thesis, 130 p. Instituto de Geociências, Universidade de Brasília, Brasília, Brazil. https://repositrio.unb.br/handle/10482/16333.
Pena, G.S., 1975. Projeto Goiânia II. Relatório Final. Relatório final. CPRM, Goiânia, 5 v.
Pena, G.S., Figueiredo, A.J.D.A., 1972. Projeto Alcalinas. Relatório final. CPRM, Goiânia, 3 v.
Peyve, A.A., 2010. Tectonics and magmatism in eastern South America and the Brazil basin of the Atlantic in the phanerozoic. Geotectonics 44 (1), 60–75. https://doi.org/10.1134/S001685211001005X.
Phillips, J.D., 2001. Tools and techniques for the application of high resolution aeromagnetic surveys to engineering problems. Symposium on the Application of Geophysics to Engineering and Environmental Problems. Environment and Engineering Geophysical Society, pp. 1–22. https://doi.org/10.4133/1.2922846.
Pimentel, M.M., 2016. The tectonic evolution of the Neoproterozoic Brasília Belt, central Brazil: a geochronological and isotopic approach. Braz. J. Geol. 46, 67–82. https://doi.org/10.1590/2317-4889201620150004.
Pimentel, M.M., Fuck, R.A., 1992. Neoproterozoic crustal accretion in central Brazil. Geology 20 (4), 375–379. https://doi.org/10.1130/0091-7613(1992)020<0375:NCAICB>2.3.CO;2.
Pimentel, M.M., Fuck, R.A., 1994. Geocronologia Rb-Sr da porção sudoeste do Maciço de Goiás. Revista Brasileira de Geociências 24 (2), 104–111.
Pimentel, M.M., Fuck, R.A., Silva, U.J.D.R., 1996. Dados Rb-Sr e Sm-Nd da região de Jussara-Goiás-Mossâmedes (GO), e o limite entre terrenos antigos do maciço de Goiás e o arco magmático de Goiás. Revista Brasileira de Geociências 26 (2), 61–70.
Pimentel, M.M., Fuck, R.A., Fischel, D.P., 1999. Estudo isotópico Sm-Nd regional da porção central da Faixa Brasília, Goiás: implicações para idade e origem dos granulitos do Complexo Anápolis-Itauçu e rochas metassedimentares do Grupo Araxá. Revista Brasileira de Geociências 29 (2), 271–276.
Pimentel, M.M., Fuck, R.A., Jost, H., Ferreira Filho, C.F., Araujo, S.M., 2000a. The basement of the Brasilia fold belt and the Goiás magmatic arc. In: Cordani, U.G., Milani, E.J., Thomaz Filho, A., Campos, D.A. (Eds.), Proceedings of the 31st International Geological Congress on The Tectonic Evolution of South America, Rio de Janeiro, Brazil, pp. 195–229.
Pimentel, M.M., Fuck, R.A., Gioia, S.M.C.L., 2000b. The Neoproterozoic Goiás magmatic arc, central Brazil: a review and new Sm-Nd isotopic data. Revista Brasileira de Geociências 30 (1), 035–039.
Pimentel, M.M., Jost, H., Fuck, R.A., 2004. O embasamento da Faixa Brasília e o arco magmático de Goiás. Geologia do Continente Sul-Americano: evolução da obra de Fernando Flávio Marques de Almeida, pp. 355–358.
Pinto, M.L., Vidotti, R.M., 2019. Tectonic framework of the Paraná basin unveiled from gravity and magnetic data. J. South Am. Earth Sci. 90, 216–232. https://doi.org/10.1016/j.jsames.2018.12.006.
Piuzana, D., Pimentel, M.M., Fuck, R.A., Armstrong, R., 2003a. Neoproterozoic granulite facies metamorphism and coeval granitic magmatism in the Brasilia Belt, Central Brazil: regional implications of new SHRIMP U–Pb and Sm–Nd data. Precambrian Res. 125 (3–4), 245–273. https://doi.org/10.1016/S0301-9268(03)00108-6.
Piuzana, D., Pimentel, M.M., Fuck, R.A., Armstrong, R., 2003b. SHRIMP U–Pb and Sm–Nd data for the Araxá Group and associated magmatic rocks: constraints for the age of sedimentation and geodynamic context of the southern Brasılia Belt, central Brazil. Precambrian Res. 125 (1–2), 139–160. https://doi.org/10.1016/S0301-9268(03)00107-4.
Reis, L.K.O., Vidotti, R.M., Cordeiro, P., Oliveira, C.G., 2020. The western São Francisco pericraton interpreted from crustal magnetic and gravity sources. J. South Am. Earth Sci. 103, 102716 https://doi.org/10.1016/j.jsames.2020.102716.
Revees, C., 2005. Aeromagnetic Surveys: Principles, Practice and Interpretation, Vol. 155. Geosoft.
Reynolds, J.M., 1997. An Introduction to Applied and Environmental Geophysics. John Wiley & Sons, p. 712.
Riccomini, C., Assumpção, M., 1999. Quaternary tectonics in Brazil. Episodes 22, 221–225.
Riccomini, C., Velázquez, V.F., Gomes, C.B., 2005. Tectonic controls of the Mesozoic and Cenozoic alkaline magmatism in central-southeastern Brazilian Platform. Mesozoic to Cenozoic alkaline magmatism in the Brazilian Platform 123, 31–56.
Ring, U., Brandon, M.T., Willett, S.D., Lister, G.S., 1999. Exhumation processes. Geol. Soc. London Spec. Publ. 154 (1), 1–27. https://doi.org/10.1144/GSL.SP.1999.154.01.01.
Rocha, M.P., Schimmel, M., Assumpção, M., 2011. Upper-mantle seismic structure beneath SE and Central Brazil from P-and S-wave regional traveltime tomography. Geophys. J. Int. 184 (1), 268–286. https://doi.org/10.1111/j.1365-246X.2010.04831.x.
Rocha, L.G.M., Pires, A.C.B., Carmelo, A.C., Araújo Filho, J.O., 2014. Geophysical characterization of the Azimuth 125° lineament with aeromagnetic data: contributions to the geology of central Brazil. Precambrian Res. 249, 273–287. https://doi.org/10.1016/j.precamres.2014.05.005.
Rocha, L.G.M., Pires, A.C.B., Carmelo, A.C., Oksum, E., 2015. Curie surface of the alkaline provinces of Goiás (GAP) and Alto Paranaiba (APAP), central Brazil. J. Volcanol. Geotherm. Res. 297, 28–38. https://doi.org/10.1016/j.jvolgeores.2015.03.006.
Rocha, M.P., de Azevedo, P.A., Marotta, G.S.A., Schimmel, M., Fuck, R., 2016. Causes of intraplate seismicity in central Brazil from travel time seismic tomography. Tectonophysics 680, 1–7. https://doi.org/10.1016/j.tecto.2016.05.005.
Rocha, L.G.M., Correa, R.T., Silva, A.B., Matos, D.R., 2019a. Geophysical reassessment of the Azimuth 125° Lineament: emplacement model and propagation of its dikes. Journal of the Geological Survey of Brazil 2 (1), 87–98. https://doi.org/10.29396/jgsb.2019.v2.n1.6.
Rocha, M.P., Assumpção, M., Affonso, G.M.P.C., Azevedo, P.A., Bianchi, M., 2019b. Teleseismic P wave tomography beneath the Pantanal, Paraná, and chaco-paraná basins, SE South America: delimiting lithospheric blocks of the SW gondwana assemblage. J. Geophys. Res. Solid Earth 124 (7), 7120–7137. https://doi.org/10.1029/2018JB016807.

Rodrigues, J.B., Gioia, S.M.L.C., Pimentel, M.M., 1999. Geocronologia e geoquímica de ortognaisses da região entre Iporá e Firminópolis: implicações para a evolução do Arco Magmático de Goiás. Revista Brasileira de Geociências 29 (2), 207–216.
Sadowski, G.R., 1987. A possible relation between pulses of platform activation and plate kinematics. Tectonophysics 143 (1-3), 43–57. https://doi.org/10.1016/0040-1951(87)90077-1.
Schobbenhaus, C., Gonçalves, J.H., Santos, J.O.S., Abram, M.B., Leão Neto, R., Matos, G.M.M., Vidotti, R.M.M., Ramos, A.B., Jesus, J.A.D. (Eds.), 2004. Carta Geológica do Brasil ao Milionésimo, Sistema de Informações Geográficas—SIG, 41 CD-ROMs, Escala 1:1.000.000. CPRM, Brasília, DF, Brazil.
Silva, M.F., 2018. Evolução tectônica de rifte para margem passiva da faixa Paraguai, 194 p. Tese (Doutorado). Instituto de Geociências, Universidade de Brasília, Brasília. http://rigeo.cprm.gov.br/jspui/handle/doc/20991.
Soares, J.E., Berrocal, J., Fuck, R.A., Mooney, W.D., Ventura, D.B., 2006. Seismic characteristics of central Brazil crust and upper mantle: a deep seismic refraction study. J. Geophys. Res. Solid Earth 111 (B12). https://doi.org/10.1029/2005JB003769.
Sousa, E.M.D., 2017. Arcabouço estrutural da porção sul da Bacia do Bananal e reativações transbrasilianas. xiv, 89 f., il. Dissertação (Mestrado em Geociências Aplicadas). Universidade de Brasília, Brasília. https://repositorio.unb.br/handle/10482/32234.
Spector, A., Grant, F.S., 1970. Statistical methods for interpreting aeromagnetic data. Geophysics 35 (2), 293–302. https://doi.org/10.1190/1.1440092.
Spector, A., Parker, W., 1979. Computer compilation and interpretation of geophysical data. In: Hood, P.J. (Ed.), Geophysics and Geochemistry in the Search for Metallic Ores: Geological Survey of Canada, Economic Geology Report Vol. 31, 527–544.
Syberg, F.J.R., 1972. A Fourier method for the regional-residual problem of potential fields. Geophys. Prospect 20 (1), 47–75. https://doi.org/10.1111/j.1365-2478.1972.tb00619.x.
Telford, W.M., Geldart, L.P., Sheriff, R.E., 1990. Applied Geophysics, 2nd. Cambridge university press. 774 p.
Teyssier, C., 2011. Exhumation of deep orogenic crust. Lithosphere 3 (6), 439–443. https://doi.org/10.1130/RF.L002.1.
Thompson, R.N., Gibson, S.A., Mitchell, J.G., Dickin, A.P., Leonardos, O.H., Brod, J.A., Greenwood, J.C., 1998. Migrating cretaceous–eocene magmatismin the serra do mar Alkaline Province, SE Brazil: melts from the deflected trindade mantle plume? J. Petrol. 39 (8), 1493–1526. https://doi.org/10.1093/petroj/39.8.1493.
Ulbrich, H.H.G.J., Gomes, C.D.B., 1981. Alkaline rocks from continental Brazil. Earth. Rev. 17 (1–2), 135–154. https://doi.org/10.1016/0012-8252(81)90009-X.
Ussami, N., Molina, E.C., 1999. Flexural modeling of the Neoproterozoic Araguaia belt, central Brazil. J. South Am. Earth Sci. 12 (1), 87–98. https://doi.org/10.1016/S0895-9811(99)00007-3.
Valeriano, C.D.M., Dardenne, M.A., Fonseca, M.A., Simões, L.S.A., Seer, H.J., 2004. A evolução tectônica da Faixa Brasília. In: Mantesso-Neto, V., Bartorelli, A., Carneiro, C.D.R., Brito Neves, B.B. (Eds.), Geologia do continente sul-americano: evolução da obra de Fernando Flávio Marques de Almeida, São Paulo, Beca, pp. 575–592.
Valeriano, C.D.M., Pimentel, M.M., Heilbron, M., Almeida, J.C.H., Trouw, R.A.J., 2008. Tectonic evolution of the Brasília Belt, Central Brazil, and early assembly of Gondwana. Geol. Soc. Lond. Spec. Publ. 294 (1), 197–210. https://doi.org/10.1144/SP294.11.
Velázquez, V.F., Gomes, C.B., Orué, D., e Comin-Chiaramonti, P., 1996. Magmatismo alcalino do Paraguai: uma revisão e atualização das províncias. Boletim IG-USP. Série Científica, 27, pp. 61–79. https://doi.org/10.11606/issn.2316-8986.v27i0p61-79.
Viana, M.D.G., Pimentel, M.M., Whitehouse, M.J., Fuck, R.A., Machado, N., 1995. O arco magmático de Mara Rosa, Goiás: Geoquímica e geocronologia e suas implicações regionais. Revista Brasileira de Geociências 25 (2), 111–123.
Zhang, J., Mattinson, C., Yu, S., Li, Y., Yu, X., Mao, X., Lu, Z., Peng, Y., 2018. Two contrasting accretion v. Collision orogenies: insights from Early Paleozoic polyphase metamorphism in the Altun–qilian–north Qaidam orogenic system, NW China. Geol. Soc. London Spec. Publ. 474 (1), 153–181. https://doi.org/10.1144/SP474.8.
Zheng, Y.F., Zhao, Z.F., Chen, R.X., 2020. Ultrahigh-pressure metamorphic rocks in the Dabie–sulu orogenic belt: compositional inheritance and metamorphic modification. Geol. Soc. Lond. Spec. Publ. 474 (1), 89–132. https://doi.org/10.1144/SP474.9.